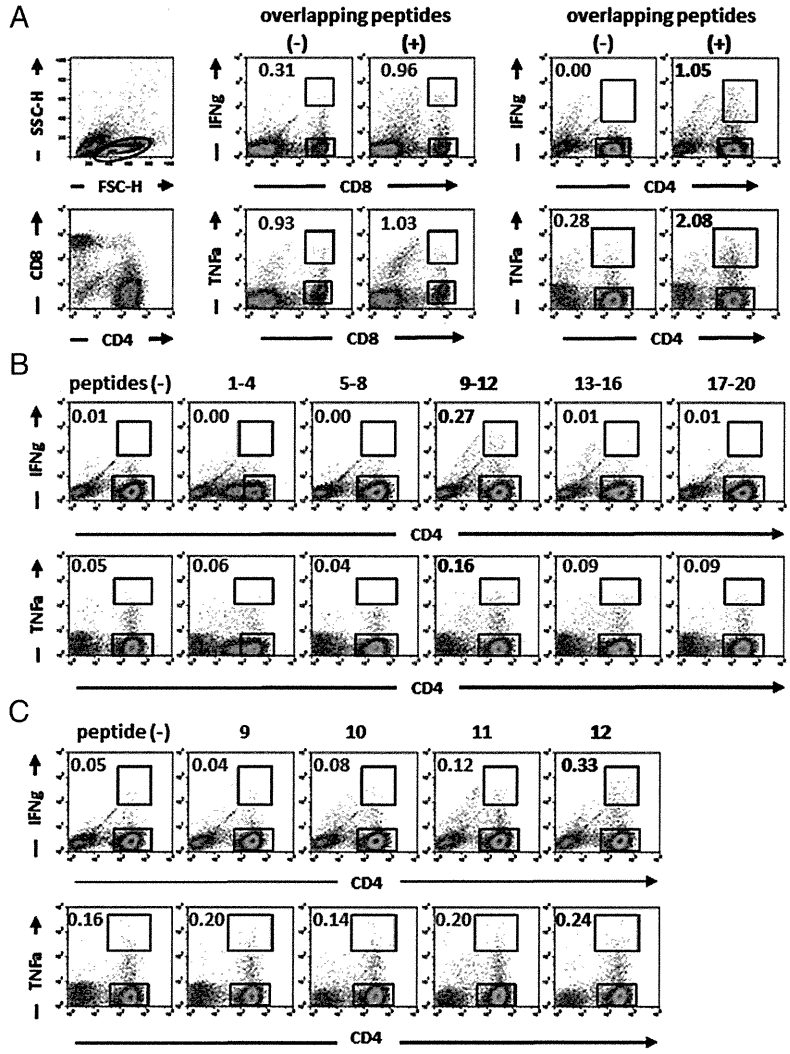

FIGURE 2. T cell responses against synthetic peptides overlapping by 10 aa and covering the entire sequence of the spliced HBZ protein. (**A**) PBMCs from patient #1 after HCT were expanded by stimulating with a mixture of 19 20-mer and 1 16-mer synthetic peptides overlapping by 10 aa and covering the entire sequence of the spliced HBZ protein. The responses of expanded CD8 and CD4 T cells to each of the overlapping peptides were evaluated by the production of IFN-γ or TNF-α. The percentage of responding cells in the upper gate ($CD8^+$ or $CD4^+$ and IFN-γ^+ or TNF-α^+ cells) relative to the cells in the lower gate ($CD8^+$ or $CD4^+$ and IFN-γ^- or TNF-α^- cells) is indicated in each flow cytometry panel. (**B**) PBMCs from patient #1 after HCT were expanded by stimulating with five overlapping peptide mixtures consisting of peptides 1–4, 5–8, 9–12, 13–16, and 17–20. (**C**) PBMCs from patient #1 after HCT were expanded by stimulating with four synthetic peptides: 9, 10, 11, and 12. The responses of expanded CD4 T cells to each synthetic peptide were evaluated by the production of IFN-γ or TNF-α. The percentage of responding cells in the upper gate relative to the cells in the lower gate is indicated in each flow cytometry panel. Each result is representative of three independent experiments.

by producing both IFN-γ and TNF-α. These cells did not respond to peptides 12-5, 12-6, or 12-7 (Fig. 3B). These data indicate that the N terminus of the minimum epitope sequence of HBZ recognized by the CD4 T cells from the patient is arginine, located at HBZ114 (Fig. 3A). Because the expanded CD4 T cells responded to peptide 12-4, the C terminus of the minimum epitope sequence of HBZ must be inside of alanine, located at HBZ125.

Next, three synthetic peptides (12-4-1, 12-4-2, 12-4-3; sequences were HBZ114–124, HBZ114–123, and HBZ114–122, respectively) were prepared to determine the C terminus of the minimum epitope sequence of HBZ (Fig. 3C). The expanded CD4 T cells responded to peptides 12-1 and 12-4 (positive controls) but not to 12-4-1, 12-4-2, 12-4-3, or a negative control peptide 12-7 (Fig. 3D). These data demonstrate that the minimum epitope sequence of HBZ recognized by the CD4 T cells from the patient was RRRAEKKAADVA (HBZ114–125).

Determination of the HLA allele on which the identified HBZ-derived peptides are presented to CD4 T cells

We investigated whether HBZ-specific CD4 T cells also recognized naturally processed and presented peptides. Thus, we initially determined *HBZ* expression by ATL or HTLV-1–immortalized cell lines and found that it was expressed by all of the lines tested (ATN-1, MT-1, MT-2, MT-4, TL-Su, TL-Om1, ATL102), regardless of their *Tax* mRNA expression (Fig. 4A, below the graph). *HBZ* expression levels of these established lines were almost as high as those of PBMCs containing >50% ATL cells obtained from 12 patients with the acute or chronic type of disease. K562 did not express *HBZ*, as might be expected, and all primary ATL cells tested were HBZ^+, consistent with an earlier study (Fig. 4A) (25). Next, we assessed the expression of HLA class II by the cell lines. The ATL or HTLV-1–immortalized cell lines tested were all positive for both HLA-DR and HLA-DQ (Fig. 4B). These observations indicate that ATN-1, MT-1, MT-2, MT-4, TL-Su, TL-Om1, and ATL102 had the potential to present the HBZ-derived peptides on their HLA-DR or HLA-DQ molecules.

Next, we examined the responses of HBZ-specific CD4 T cells from patient #1 after HCT against K562 or HBZ-expressing lines of different HLA types. The responses of HBZ-specific CD4 T cells to the lines were evaluated without the addition of peptide. The CD4 T cells that had been expanded from patient #1 after HCT using peptide 12 responded to peptide 12-1 (positive control) but not to K562, which expressed no *HBZ* (negative control) (Fig. 4C, *upper six panels*). When tested against ATL or HTLV-1–immortalized cell lines, the CD4 T cells responded strongly to ATN-1 and TL-Su (Fig. 4C, *lower panels*). Comparing the HLA class II types of the donor of the effector CD4 T cells (patient #1 after HCT) with ATN-1 and TL-Su showed that HLA-DRB1*15:01 and

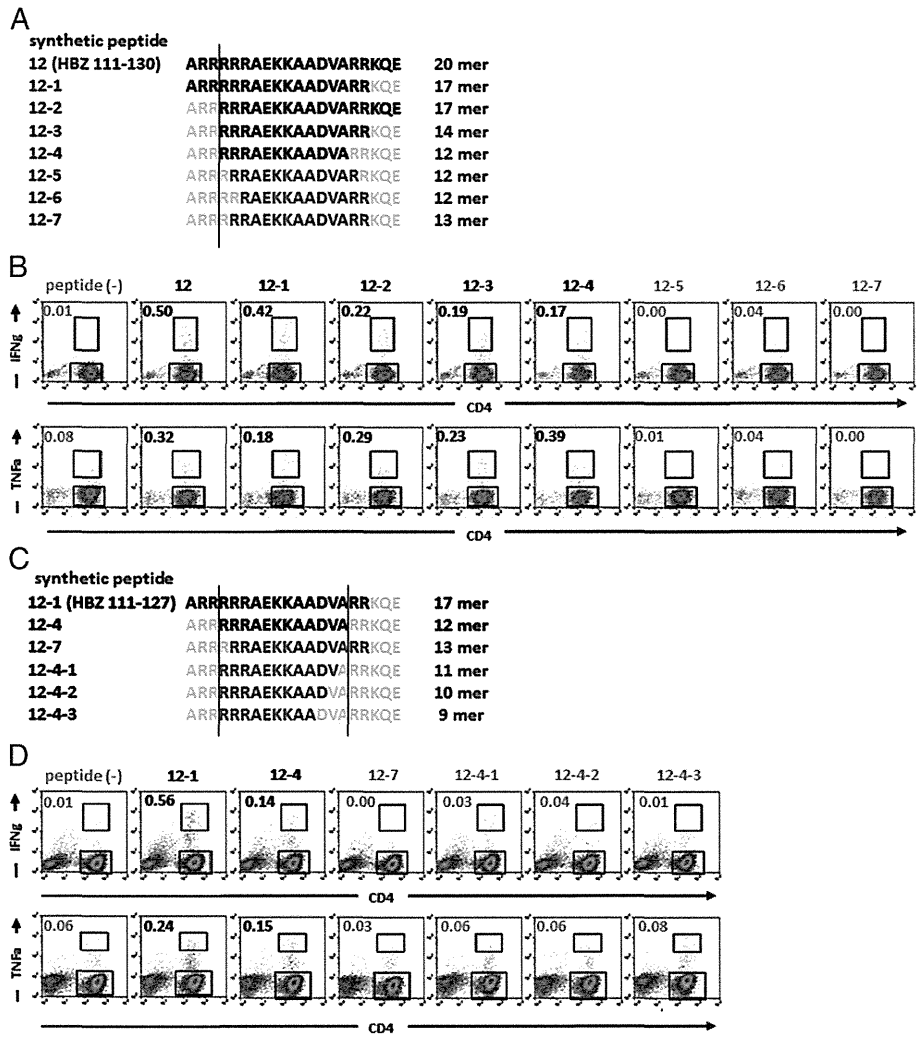

FIGURE 3. Determination of the minimum epitope sequence of HBZ recognized by CD4 T cells. (**A**) Schematic diagram of seven synthetic peptides (12-1, 12-2, 12-3, 12-4, 12-5, 12-6, 12-7) from peptide 12. They were prepared to determine the N terminus of the sequence representing the minimum epitope of HBZ recognized by the CD4 T cells. (**B**) PBMCs from patient #1 after HCT were expanded by peptide 12. The responses of expanded CD4 T cells to each synthetic peptide (12, 12-1, 12-2, 12-3, 12-4, 12-5, 12-6, 12-7) were evaluated by the production of IFN-γ or TNF-α. The percentage of responding cells in the upper gate relative to the cells in the lower gate is indicated in each flow cytometry panel. Each result is representative of three independent experiments. (**C**) Schematic diagram of three synthetic peptides (12-4-1, 12-4-2, 12-4-3) prepared to determine the C terminus of the sequence representing the minimum epitope of HBZ recognized by the CD4 T cells. (**D**) The responses of expanded CD4 T cells to each synthetic peptide (12-1, 12-4, 12-7, 12-4-1, 12-4-2, 12-4-3) were evaluated by the production of IFN-γ or TNF-α. The percentage of responding cells in the upper gate relative to the cells in the lower gate is indicated in each flow cytometry panel. Each result is representative of three independent experiments.

HLA-DQB1*06:02 were shared by all three (Table I). In addition, the CD4 T cells responded to MT-2, TL-Om1, and ATL102 to a lesser degree (Fig. 4C, *lower panels*); these three lines were found to share HLA-DRB1*15:02 and HLA-DQB1*06:01 (Table I). Together, these results indicate that the HBZ-specific CD4 T cell responses from patient #1 after HCT were restricted by HLA-DRB1*15:01 or HLA-DQB1*06:02, as well as by HLA-DRB1*15:02 or HLA-DQB1*06:01. In contrast, the peptide-sensitized CD4 T cells did not respond to MT-1 or MT-4 (Fig. 4C, *lower panels*), consistent with the present observations that the epitope of HBZ recognized by such CD4 T cells was restricted by HLA-DRB1*15:01/HLA-DQB1*06:02 and HLA-DRB1*15:02/HLA-DQB1*06:01.

Next, we tested whether HLA-DR or HLA-DQ restricted the presentation of the HBZ-derived peptide. CD4 T cells expanded by peptide 12 no longer responded to specific stimulation by peptide 12 in the presence of anti–HLA-DR–blocking mAb by producing IFN-γ (Fig. 5A, *upper left panels*), but it did respond in the presence of the isotype-control mAb (Fig. 5A, *upper right panels*). These CD4 T cells also still responded to peptide 12 in the presence of anti–HLA-DQ–blocking mAb (Fig. 5A, *lower left panels*) and its isotype control (Fig. 5A, *lower right panels*). In addition, in the presence of anti–HLA-DR–blocking mAb, CD4 T cells expanded by peptide 12 no longer responded to ATN-1 (Fig. 5B, *left panels*), which carried HLA-DRB1*15:01/HLA-DQB1*06:02 (Table I) and expressed *HBZ* mRNA (Fig. 4A). However, they did respond by producing IFN-γ and TNF-α in the presence of the isotype control (Fig. 5B, *left panels*). These CD4 T cells also still responded to ATN-1 in the presence of anti–HLA-DQ–blocking mAb and its isotype control (Fig. 5B, *right panels*). Furthermore, HBZ-specific CD4 T cell responses to K562 (negative control) were not affected by anti–HLA-DR, anti–HLA-DQ, or their isotype mAbs (Fig. 5C). These observations from Ab-blocking experiments, together with the results shown in Fig. 4, indicate that the epitope sequence of HBZ recognized by the CD4 T cells from patient #1 after HCT were restricted by HLA-DR, specifically HLA-DRB1*15:01 and HLA-DRB1*15:02.

Clinical significance of the specific CD4 T cell response against HBZ

The data presented thus far pertained to CD4 T cells obtained from only one patient (patient #1 after HCT). Therefore, we used HBZ peptide 12 to stimulate and expand 28 PBMC samples obtained from 27 other HTLV-1–infected individuals who carried HLA-DRB1*15:01 or HLA-DRB1*15:02. PBMCs were obtained from 10 HTLV-1 ACs, 10 ATL patients who had not undergone allogeneic HCT, and 8 ATL patients after allogeneic HCT. Among them, PBMCs from one individual (patient #2) were tested at different disease stages (i.e., CRs before and after allogeneic HCT). HBZ-specific CD4 T cell responses were absent in all 10

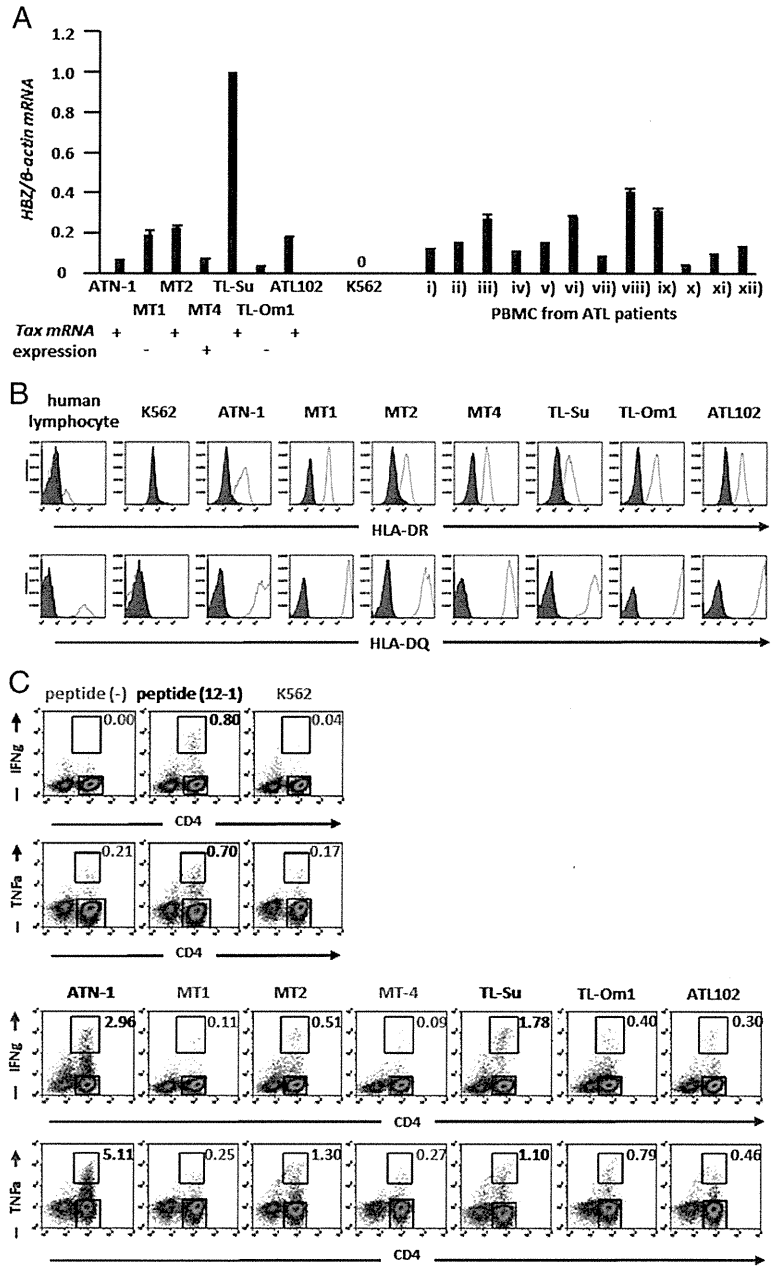

FIGURE 4. Responses of HBZ-specific CD4 T cells from patient #1 after HCT to ATL or HTLV-1–immortalized cell lines. (**A**) *HBZ* expression in ATL and HTLV-1–immortalized cell lines, K562, or PBMCs from ATL patients was analyzed by qRT-PCR by dividing the *HBZ* expression level by the *β-actin* expression level, resulting in an *HBZ/β-actin* mRNA ratio with the expression level in TL-Su set at unity. Data shown are means of triplicate experiments; error bars represent SD. *Tax* mRNA expression of each ATL and HTLV-1–immortalized cell line is indicated, as determined in our previous study (8). (**B**) HLA-DR and HLA-DQ expression in ATL cell lines, HTLV-1–immortalized lines, or K562, as analyzed by flow cytometry. The cell lines were stained with anti–HLA-DR mAb (*upper panels*, open graphs), anti–HLA-DQ mAb (*lower panels*, open graphs), or the corresponding isotype-control mAbs (filled graphs). (**C**) The expanded CD4 T cells were cocultured or not with the synthetic peptide 12-1. Negative controls without peptide stimulation (*upper left panels*) and positive controls with peptide stimulation (*upper middle panels*) are shown. The expanded CD4 T cells were cocultured with target cell lines in the absence of peptide stimulation. CD4 T cells did not respond to K562, which expressed no HBZ and acted as the negative control (*upper right panels*). The CD4 T cell responses to ATL or HTLV-1–immortalized cell lines, which expressed *HBZ*, with different HLA types were evaluated (*lower panels*). The percentage of responding cells in the upper gate relative to the cells in the lower gate is indicated in each flow cytometry panel. Each result is representative of three independent experiments.

HTLV-1 ACs, as well as in all 10 nontransplanted ATL patients (of whom 9 were in CR after systemic chemotherapy and the other was of smoldering type under observation only). In contrast, specific CD4 T cell responses to HBZ were observed in three of the eight additional ATL patients who were in CR after allogeneic HCT (patients #2, #3, and #4). The CD4 T cells from patient #2 and #4 after HCT responded to HBZ peptide 12 by producing both IFN-γ and TNF-α (Fig. 6, *right panels*). In patient #3, no TNF-α response was observed, but there was a clear IFN-γ response to HBZ peptide 12 (Fig. 6, *lower left panels*). Thus, specific CD4 T cell responses against HBZ were observed in four of nine recipients after allogeneic HCT (44%) but in no other ATL patients. Among the patients examined in this study, one patient with acute-type ATL received systemic chemotherapy and achieved CR. Subsequently, she received allogeneic HCT from an HLA-A, B, DR-matched HTLV-1 noninfected sibling donor and maintained CR (patient #2 after HCT). Although HBZ-specific CD4 T cell responses were not present at CR before allogeneic HCT in this patient (Fig. 6, *upper left panels*), they developed after transplantation (Fig. 6, *upper right panels*).

Table I. HLA information

	HLA-DRB1		HLA-DQB1		HLA-DPB1	
ATN-1	*04:05	*15:01	*04:01	*06:02	*05:01	*05:01
MT-1	*04:01	*09:01	*03:01	*03:03	*04:02	*05:01
MT-2	*04:04	*15:02	*03:02	*06:01	*05:01	*09:01
MT-4	*01:01	*16:02	*05:01	*05:02	*05:01	*05:01
TL-Su	*09:01	*15:01	*03:03	*06:02	*02:01	*17:01
TL-Om1	*15:02	*15:02	*06:01	*06:01	*09:01	*09:01
ATL102	*04:04	*15:02	*03:02	*06:01	*05:01	*09:01
Patient #1 after HCT	*04:05	*15:01	*04:01	*06:02	*02:01	*06:01

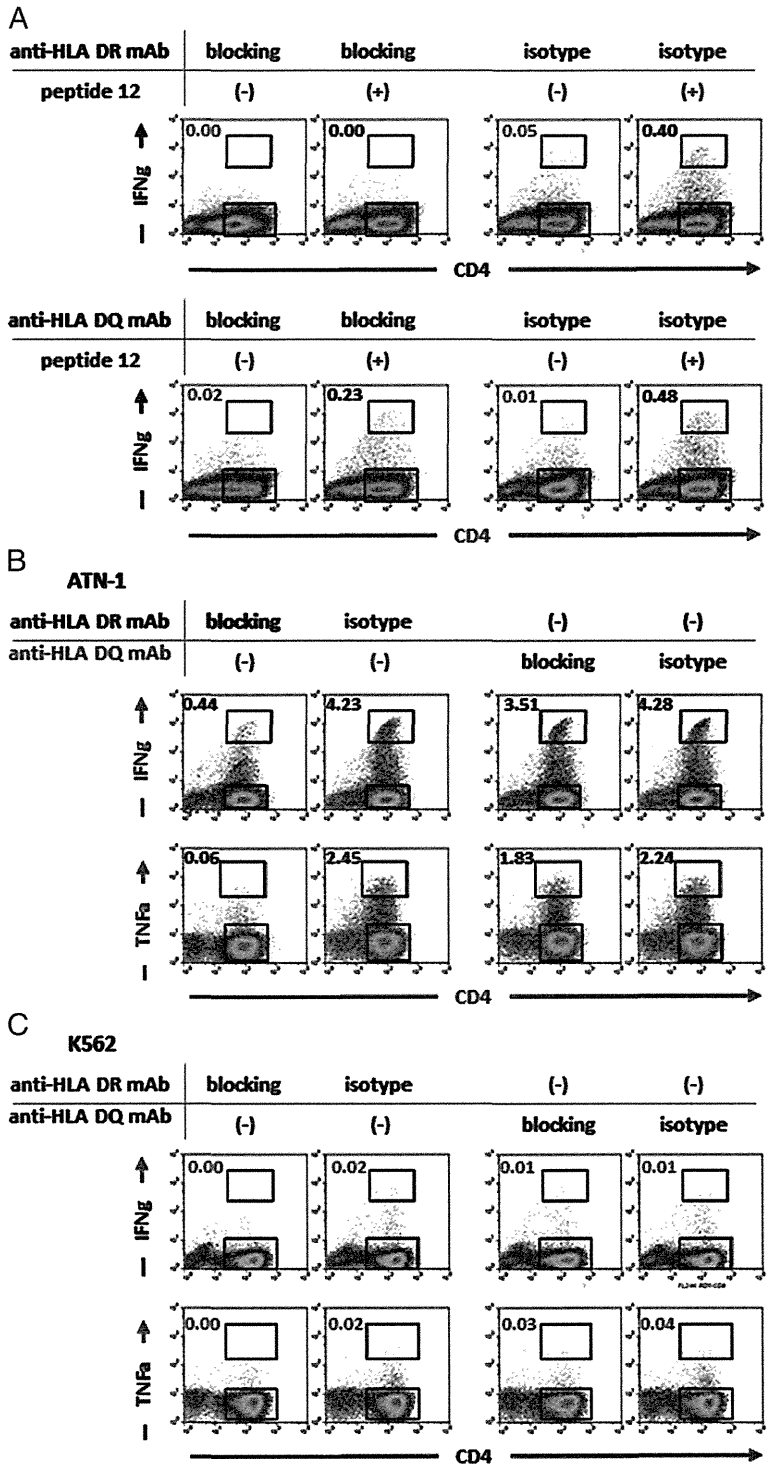

FIGURE 5. Determination of the HLA alleles restricting the presentation of HBZ-derived peptides to HBZ-specific CD4 T cells. (**A**) Responses of HBZ-specific CD4 T cells were evaluated, with or without HBZ peptide 12, in the presence of anti–HLA-DR–blocking mAb (*upper left panels*), anti–HLA-DQ–blocking mAb (*lower left panels*), or the corresponding isotype-control mAb (anti-HLA-DR isotype mAb, *upper right panels*; anti-HLA-DQ isotype mAb, *lower right panels*). Responses of HBZ-specific CD4 T cells to ATN-1, which carries HLA-DRB1*15:01/HLA-DQB1*06:02 and expresses *HBZ* mRNA (**B**), and to K562 (negative control) (**C**) were also evaluated in the presence of HLA-blocking mAbs or their isotype controls, without peptide stimulation. The percentage of responding cells in the upper gate relative to the cells in the lower gate is indicated in each flow cytometry panel. Each result is representative of three independent experiments.

Discussion

In the current study, we demonstrated the presence of HBZ-specific CD4 T cells in an ATL patient after allogeneic HCT and determined the minimum sequence of a novel HLA-DRB1*15:01–restricted HBZ-derived epitope to be RRRAEKKAADVA (HBZ114–125). HBZ peptides including the sequence HBZ114–125 were also presented on HLA-DRB1*15:02 and recognized by CD4 T cells. To the best of our knowledge, this is the first report to identify naturally processed and presented HLA-DR–restricted epitopes derived from HBZ on the surface of ATL cells. In an earlier study, an HBZ peptide–specific CTL line was established from an HLA-A*02:01^{+} individual, using peptides derived from the HBZ sequence. The peptides were selected by computer algorithms available at the BioInformatics and Molecular Analysis Section Web site (http://www-bimas.cit.nih.gov/molbio/hla_bind/) and the SYFPEITHI Web site (http://www.syfpeithi.de/) for strong binding affinity to the HLA-A*02:01 molecule. However, the established CTL line recognized the corresponding peptide-pulsed

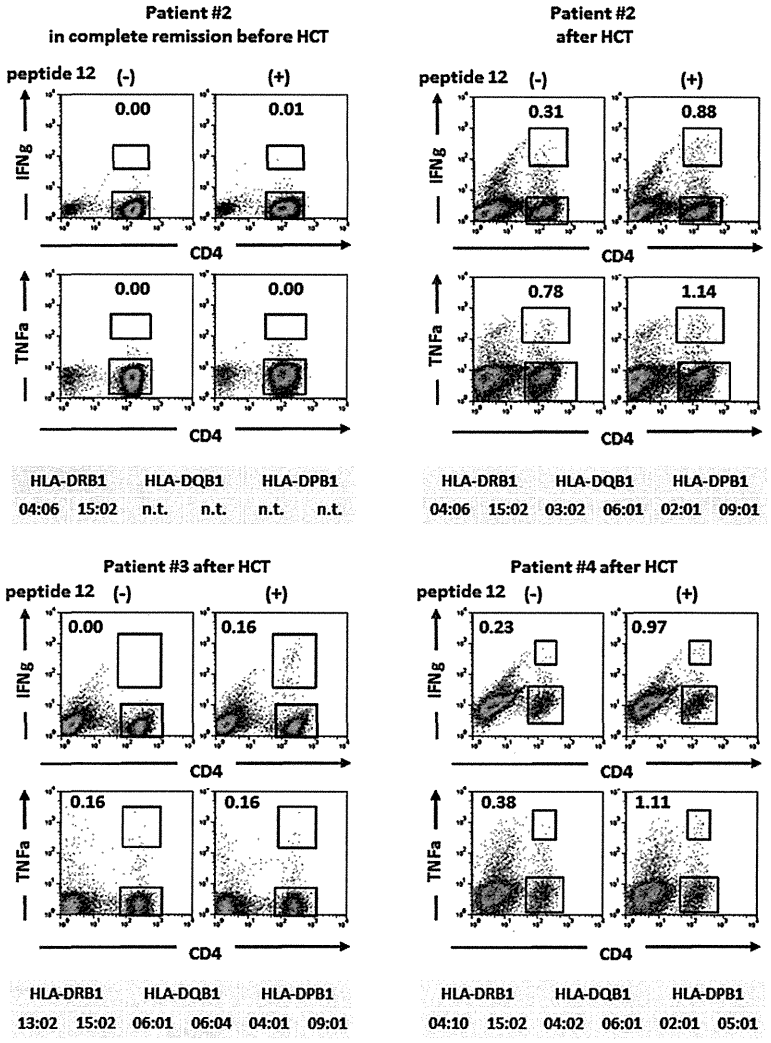

FIGURE 6. HBZ-specific CD4 T cell responses in additional ATL patients. PBMCs from additional ATL patients (#2, #3, and #4) carrying HLA-DRB1*15:02 were expanded by stimulation with HBZ peptide 12. The responses of expanded CD4 T cells to peptide 12 were evaluated by the production of IFN-γ or TNF-α. Although no HBZ-specific CD4 T cell response was observed in patient #2 in CR before allogeneic HCT (*upper left panels*), they developed after transplantation (*upper right panels*). HBZ-specific CD4 T cell responses were also observed in patient #3 (*lower left panels*) and patient #4 (*lower right panels*) in CR after allogeneic HCT. The percentage of responding cells in the upper gate relative to the cells in the lower gate is indicated in each flow cytometry panel. The HLA type of each patient is indicated below the flow cytometry panels. Each result is representative of three independent experiments. n.t., Not tested.

HLA-A*02:01$^+$ cells but not ATL cells (29). Therefore, it was not determined whether HBZ-derived peptides could be naturally presented on cells from HTLV-1–infected people. Another earlier study (30) demonstrated that HBZ expression was a critical determinant of viral persistence in the chronic phase of HTLV-1 infection. That novel study was performed using experimentally validated epitope-prediction software (34), but it did not determine the HBZ-derived epitope sequence or the corresponding HLA allele presenting it.

In the current study, no HLA-DRB1*15:01–restricted or HLA-DRB1*15:02–restricted HBZ-specific CD4 T cell response was observed in any ATL patients who had not undergone allogeneic HCT or in any HTLV-1 ACs. We surmise that HTLV-1 transmission from mothers to infants through breast milk in early life induces tolerance to HBZ, but not to Tax, by unknown mechanisms, resulting in insufficient HBZ-specific T cell responses in HTLV-1–infected individuals. This would be consistent with the persistent expression of HBZ in HTLV-1–infected cells (2, 25). In addition, insufficient HBZ-specific T cell responses may be due, in part, to the fact that the majority of the *HBZ* mRNA is retained in the nucleus, which may inhibit its translation (35), and probably leads to a low level of HBZ protein expression in HTLV-1–infected cells (29). In contrast, the finding that HLA-DRB1*15:01–restricted or HLA-DRB1*15:02–restricted HBZ-specific CD4 T cell responses were detected in ATL patients after allogeneic HCT requires explanation. Our hypothesis is that, after allogeneic HCT, the reconstituted immune system from donor-derived hematopoietic stem cells can recognize virus protein HBZ as foreign, although its expression is low, and HBZ-specific immune responses are provoked because of the lack of tolerance induction under these circumstances. In one patient with acute-type disease, HBZ-specific CD4 T cell responses were not observed in PBMCs at the time of CR before HCT, but they became detectable after allogeneic HCT. This observation supports our hypothesis. An earlier study (36) reported that HBZ-specific T cell responses were detected in some patients with HTLV-1–associated myelopathy (HAM). Unlike ATL, HAM can occur in individuals infected with HTLV-1 by any route of transmission, such as sexual intercourse (37). Therefore, some patients with HAM, infected with HTLV-1 after reaching adulthood (i.e., who became infected after their immune system had fully matured), may recognize virus protein HBZ as foreign, and HBZ-specific immune responses may be provoked. From this point of view, detection of HBZ-specific T cell responses might be expected in some HTLV-1 ACs, infected after becoming adults, but we did not see this in the present study.

In conclusion, we report the presence of HBZ-specific CD4 T cell responses in ATL patients who were in CR but only after allogeneic HCT. These responses potentially contribute to the

graft-versus-HTLV-1 effect. Novel strategies that enhance the posttransplantation allogeneic anti–HTLV-1 effect targeting HBZ, which never provokes graft-versus-host disease, could lead to improved outcomes of allogeneic HCT for ATL.

Acknowledgments

We thank Chiori Fukuyama for excellent technical assistance and Naomi Ochiai for excellent secretarial assistance.

Disclosures

T.I. received honoraria from Kyowa Hakko Kirin. The other authors have no financial conflicts of interest.

References

1. Uchiyama, T., J. Yodoi, K. Sagawa, K. Takatsuki, and H. Uchino. 1977. Adult T-cell leukemia: clinical and hematologic features of 16 cases. *Blood* 50: 481–492.
2. Matsuoka, M., and K. T. Jeang. 2007. Human T-cell leukaemia virus type 1 (HTLV-1) infectivity and cellular transformation. *Nat. Rev. Cancer* 7: 270–280.
3. Ishida, T., and R. Ueda. 2011. Antibody therapy for Adult T-cell leukemia-lymphoma. *Int. J. Hematol.* 94: 443–452.
4. Tsukasaki, K., T. Maeda, K. Arimura, J. Taguchi, T. Fukushima, Y. Miyazaki, Y. Moriuchi, K. Kuriyama, Y. Yamada, and M. Tomonaga. 1999. Poor outcome of autologous stem cell transplantation for adult T cell leukemia/lymphoma: a case report and review of the literature. *Bone Marrow Transplant.* 23: 87–89.
5. Utsunomiya, A., Y. Miyazaki, Y. Takatsuka, S. Hanada, K. Uozumi, S. Yashiki, M. Tara, F. Kawano, Y. Saburi, H. Kikuchi, et al. 2001. Improved outcome of adult T cell leukemia/lymphoma with allogeneic hematopoietic stem cell transplantation. *Bone Marrow Transplant.* 27: 15–20.
6. Ishida, T., M. Hishizawa, K. Kato, R. Tanosaki, T. Fukuda, S. Taniguchi, T. Eto, Y. Takatsuka, Y. Miyazaki, Y. Moriuchi, et al. 2012. Allogeneic hematopoietic stem cell transplantation for adult T-cell leukemia-lymphoma with special emphasis on preconditioning regimen: a nationwide retrospective study. *Blood* 120: 1734–1741.
7. Akimoto, M., T. Kozako, T. Sawada, K. Matsushita, A. Ozaki, H. Hamada, H. Kawada, M. Yoshimitsu, M. Tokunaga, K. Haraguchi, et al. 2007. Anti-HTLV-1 tax antibody and tax-specific cytotoxic T lymphocyte are associated with a reduction in HTLV-1 proviral load in asymptomatic carriers. *J. Med. Virol.* 79: 977–986.
8. Suzuki, S., A. Masaki, T. Ishida, A. Ito, F. Mori, F. Sato, T. Narita, M. Ri, S. Kusumoto, H. Komatsu, et al. 2012. Tax is a potential molecular target for immunotherapy of adult T-cell leukemia/lymphoma. *Cancer Sci.* 103: 1764–1773.
9. Masaki, A., T. Ishida, S. Suzuki, A. Ito, F. Mori, F. Sato, T. Narita, T. Yamada, M. Ri, S. Kusumoto, et al. 2013. Autologous Tax-specific CTL therapy in a primary adult T cell leukemia/lymphoma cell-bearing NOD/Shi-scid, IL-2Rγnull mouse model. *J. Immunol.* 191: 135–144.
10. Harashima, N., K. Kurihara, A. Utsunomiya, R. Tanosaki, S. Hanabuchi, M. Masuda, T. Ohashi, F. Fukui, A. Hasegawa, T. Masuda, et al. 2004. Graft-versus-Tax response in adult T-cell leukemia patients after hematopoietic stem cell transplantation. *Cancer Res.* 64: 391–399.
11. Tamai, Y., A. Hasegawa, A. Takamori, A. Sasada, R. Tanosaki, I. Choi, A. Utsunomiya, Y. Maeda, Y. Yamano, T. Eto, et al. 2013. Potential contribution of a novel Tax epitope-specific CD4+ T cells to graft-versus-Tax effect in adult T cell leukemia patients after allogeneic hematopoietic stem cell transplantation. *J. Immunol.* 190: 4382–4392.
12. Nishikawa, H., Y. Maeda, T. Ishida, S. Gnjatic, E. Sato, F. Mori, D. Sugiyama, A. Ito, Y. Fukumori, A. Utsunomiya, et al. 2012. Cancer/testis antigens are novel targets of immunotherapy for adult T-cell leukemia/lymphoma. *Blood* 119: 3097–3104.
13. Itonaga, H., H. Tsushima, J. Taguchi, T. Fukushima, H. Taniguchi, S. Sato, K. Ando, Y. Sawayama, E. Matsuo, R. Yamasaki, et al. 2013. Treatment of relapsed adult T-cell leukemia/lymphoma after allogeneic hematopoietic stem cell transplantation: the Nagasaki Transplant Group experience. *Blood* 121: 219–225.
14. Ishida, T., M. Hishizawa, K. Kato, R. Tanosaki, T. Fukuda, Y. Takatsuka, T. Eto, Y. Miyazaki, M. Hidaka, N. Uike, et al. 2013. Impact of Graft-versus-Host Disease on Allogeneic Hematopoietic Cell Transplantation for Adult T Cell Leukemia-Lymphoma Focusing on Preconditioning Regimens: Nationwide Retrospective Study. *Biol. Blood Marrow Transplant.* 19: 1731–1739.
15. Poiesz, B. J., F. W. Ruscetti, A. F. Gazdar, P. A. Bunn, J. D. Minna, and R. C. Gallo. 1980. Detection and isolation of type C retrovirus particles from fresh and cultured lymphocytes of a patient with cutaneous T-cell lymphoma. *Proc. Natl. Acad. Sci. USA* 77: 7415–7419.
16. Hinuma, Y., K. Nagata, M. Hanaoka, M. Nakai, T. Matsumoto, K. I. Kinoshita, S. Shirakawa, and I. Miyoshi. 1981. Adult T-cell leukemia: antigen in an ATL cell line and detection of antibodies to the antigen in human sera. *Proc. Natl. Acad. Sci. USA* 78: 6476–6480.
17. Gonçalves, D. U., F. A. Proietti, J. G. Ribas, M. G. Araújo, S. R. Pinheiro, A. C. Guedes, and A. B. Carneiro-Proietti. 2010. Epidemiology, treatment, and prevention of human T-cell leukemia virus type 1-associated diseases. *Clin. Microbiol. Rev.* 23: 577–589.
18. Grassmann, R., C. Dengler, I. Müller-Fleckenstein, B. Fleckenstein, K. McGuire, M. C. Dokhelar, J. G. Sodroski, and W. A. Haseltine. 1989. Transformation to continuous growth of primary human T lymphocytes by human T-cell leukemia virus type I X-region genes transduced by a Herpesvirus saimiri vector. *Proc. Natl. Acad. Sci. USA* 86: 3351–3355.
19. Tanaka, A., C. Takahashi, S. Yamaoka, T. Nosaka, M. Maki, and M. Hatanaka. 1990. Oncogenic transformation by the tax gene of human T-cell leukemia virus type I in vitro. *Proc. Natl. Acad. Sci. USA* 87: 1071–1075.
20. Akagi, T., and K. Shimotohno. 1993. Proliferative response of Tax1-transduced primary human T cells to anti-CD3 antibody stimulation by an interleukin-2-independent pathway. *J. Virol.* 67: 1211–1217.
21. Hinrichs, S. H., M. Nerenberg, R. K. Reynolds, G. Khoury, and G. Jay. 1987. A transgenic mouse model for human neurofibromatosis. *Science* 237: 1340–1343.
22. Nerenberg, M., S. H. Hinrichs, R. K. Reynolds, G. Khoury, and G. Jay. 1987. The tat gene of human T-lymphotropic virus type 1 induces mesenchymal tumors in transgenic mice. *Science* 237: 1324–1329.
23. Hasegawa, H., H. Sawa, M. J. Lewis, Y. Orba, N. Sheehy, Y. Yamamoto, T. Ichinohe, Y. Tsunetsugu-Yokota, H. Katano, H. Takahashi, et al. 2006. Thymus-derived leukemia-lymphoma in mice transgenic for the Tax gene of human T-lymphotropic virus type I. *Nat. Med.* 12: 466–472.
24. Ohsugi, T., T. Kumasaka, S. Okada, and T. Urano. 2007. The Tax protein of HTLV-1 promotes oncogenesis in not only immature T cells but also mature T cells. *Nat. Med.* 13: 527–528.
25. Satou, Y., J. Yasunaga, M. Yoshida, and M. Matsuoka. 2006. HTLV-I basic leucine zipper factor gene mRNA supports proliferation of adult T cell leukemia cells. *Proc. Natl. Acad. Sci. USA* 103: 720–725.
26. Satou, Y., J. Yasunaga, T. Zhao, M. Yoshida, P. Miyazato, K. Takai, K. Shimizu, K. Ohshima, P. L. Green, N. Ohkura, et al. 2011. HTLV-1 bZIP factor induces T-cell lymphoma and systemic inflammation in vivo. *PLoS Pathog.* 7: e1001274.
27. Fan, J., G. Ma, K. Nosaka, J. Tanabe, Y. Satou, A. Koito, S. Wain-Hobson, J. P. Vartanian, and M. Matsuoka. 2010. APOBEC3G generates nonsense mutations in human T-cell leukemia virus type 1 proviral genomes in vivo. *J. Virol.* 84: 7278–7287.
28. Takeda, S., M. Maeda, S. Morikawa, Y. Taniguchi, J. Yasunaga, K. Nosaka, Y. Tanaka, and M. Matsuoka. 2004. Genetic and epigenetic inactivation of tax gene in adult T-cell leukemia cells. *Int. J. Cancer* 109: 559–567.
29. Suemori, K., H. Fujiwara, T. Ochi, T. Ogawa, M. Matsuoka, T. Matsumoto, J. M. Mesnard, and M. Yasukawa. 2009. HBZ is an immunogenic protein, but not a target antigen for human T-cell leukemia virus type 1-specific cytotoxic T lymphocytes. *J. Gen. Virol.* 90: 1806–1811.
30. Macnamara, A., A. Rowan, S. Hilburn, U. Kadolsky, H. Fujiwara, K. Suemori, M. Yasukawa, G. Taylor, C. R. Bangham, and B. Asquith. 2010. HLA class I binding of HBZ determines outcome in HTLV-1 infection. *PLoS Pathog.* 6: e1001117.
31. Enose-Akahata, Y., A. Abrams, R. Massoud, I. Bialuk, K. R. Johnson, P. L. Green, E. M. Maloney, and S. Jacobson. 2013. Humoral immune response to HTLV-1 basic leucine zipper factor (HBZ) in HTLV-1-infected individuals. *Retrovirology* 10: 19.
32. Shimoyama, M. 1991. Diagnostic criteria and classification of clinical subtypes of adult T-cell leukaemia-lymphoma. A report from the Lymphoma Study Group (1984-87). *Br. J. Haematol.* 79: 428–437.
33. Ishida, T., A. Utsunomiya, S. Iida, H. Inagaki, Y. Takatsuka, S. Kusumoto, G. Takeuchi, S. Shimizu, M. Ito, H. Komatsu, et al. 2003. Clinical significance of CCR4 expression in adult T-cell leukemia/lymphoma: its close association with skin involvement and unfavorable outcome. *Clin. Cancer Res.* 9: 3625–3634.
34. MacNamara, A., U. Kadolsky, C. R. Bangham, and B. Asquith. 2009. T-cell epitope prediction: rescaling can mask biological variation between MHC molecules. *PLOS Comput. Biol.* 5: e1000327.
35. Rende, F., I. Cavallari, A. Corradin, M. Silic-Benussi, F. Toulza, G. M. Toffolo, Y. Tanaka, S. Jacobson, G. P. Taylor, D. M. D'Agostino, et al. 2011. Kinetics and intracellular compartmentalization of HTLV-1 gene expression: nuclear retention of HBZ mRNAs. *Blood* 117: 4855–4859.
36. Hilburn, S., A. Rowan, M. A. Demontis, A. MacNamara, B. Asquith, C. R. Bangham, and G. P. Taylor. 2011. In vivo expression of human T-lymphotropic virus type 1 basic leucine-zipper protein generates specific CD8+ and CD4+ T-lymphocyte responses that correlate with clinical outcome. *J. Infect. Dis.* 203: 529–536.
37. Yamano, Y., and T. Sato. 2012. Clinical pathophysiology of human T-lymphotropic virus-type 1-associated myelopathy/tropical spastic paraparesis. *Front. Microbiol.* 3: 389.

Autologous Tax-Specific CTL Therapy in a Primary Adult T Cell Leukemia/Lymphoma Cell–Bearing NOD/Shi-*scid*, IL-2Rγ^{null} Mouse Model

Ayako Masaki,* Takashi Ishida,* Susumu Suzuki,*,† Asahi Ito,* Fumiko Mori,* Fumihiko Sato,*,‡ Tomoko Narita,* Tomiko Yamada,* Masaki Ri,* Shigeru Kusumoto,* Hirokazu Komatsu,* Yuetsu Tanaka,§ Akio Niimi,* Hiroshi Inagaki,‡ Shinsuke Iida,* and Ryuzo Ueda†

We expanded human T-lymphotropic virus type 1 Tax-specific CTL in vitro from PBMC of three individual adult T cell leukemia/lymphoma (ATL) patients and assessed their therapeutic potential in an in vivo model using NOG mice bearing primary ATL cells from the respective three patients (ATL/NOG). In these mice established with cells from a chronic-type patient, treatment by i.p. injection of autologous Tax-CTL resulted in greater infiltration of CD8-positive T cells into each ATL lesion. This was associated with a significant decrease of ATL cell infiltration into blood, spleen, and liver. Tax-CTL treatment also significantly decreased human soluble IL-2R concentrations in the sera. In another group of ATL/NOG mice, Tax-CTL treatment led to a significant prolongation of survival time. These findings show that Tax-CTL can infiltrate the tumor site, recognize, and kill autologous ATL cells in mice in vivo. In ATL/NOG mice with cells from an acute-type patient, whose postchemotherapeutic remission continued for >18 mo, antitumor efficacy of adoptive Tax-CTL therapy was also observed. However, in ATL/NOG mice from a different acute-type patient, whose ATL relapsed after 6 mo of remission, no efficacy was observed. Thus, although the therapeutic effects were different for different ATL patients, to the best of our knowledge, this is the first report that adoptive therapy with Ag-specific CTL expanded from a cancer patient confers antitumor effects, leading to significant survival benefit for autologous primary cancer cell–bearing mice in vivo. The present study contributes to research on adoptive CTL therapy, which should be applicable to several types of cancer. *The Journal of Immunology*, **2013, 191: 135–144.**

Adult T cell leukemia/lymphoma (ATL) is a distinct hematologic malignancy caused by human T-lymphotropic virus type 1 (HTLV-1) (1–4). ATL patients have a very poor prognosis for which no standard treatment strategy is available (5, 6). Over the last decade, allogeneic hematopoietic stem cell transplantation has evolved into a potential approach to treat ATL patients. However, only a small fraction of patients can benefit from transplantation, such as those who are younger, have achieved sufficient disease control, and have an appropriate stem cell source (7, 8). Therefore, the development of alternative treatment strategies for ATL patients is an urgent issue.

HTLV-1 Tax, a virus-encoded regulatory gene product, is required for the virus to transform cells (9) and is thought to be indispensable for oncogenesis. Therefore, Tax has been considered as a molecular target for immunotherapy against ATL (10–14). However, it was reported that the level of Tax expression in HTLV-1–infected cells decreases during disease progression, and *Tax* transcripts are detected only in ~40% of established ATL cases (15). Moreover, weak or absent responses to Tax were observed in ATL patients (16), leading to controversy as to whether Tax is an appropriate target for immunotherapy of ATL. In this context, we have recently reported the potential relevance of Tax as a target for ATL immunotherapy. Tax-specific CTL recognized HLA/Tax–peptide complexes on autologous ATL cells and killed them, even when their Tax expression was so low that it could only be detected by RT-PCR but not at the protein level in vitro (17). However, in general, tumors develop in a complex and dynamic microenvironment in humans (18–20). Therefore, antitumor activities of cancer-specific CTL should be evaluated under conditions including the cancer microenvironment. In addition, susceptibility to CTL is different in established cell lines and primary tumor cells isolated directly ex vivo from patients, especially autologous tumor cells, with the latter certainly being most relevant for evaluating antitumor effects of CTL. Based on these considerations, we expanded Tax-specific CTL in vitro from PBMC of ATL patients and tested in this study the potential significance of Tax as a target for ATL immunotherapy in an in vivo model consisting of NOD/Shi-*scid*, IL-2Rγ^{null} (NOG) mice (21) bearing the autologous primary ATL cells (ATL/NOG).

*Department of Medical Oncology and Immunology, Nagoya City University Graduate School of Medical Sciences, Aichi 467-8601, Japan; †Department of Tumor Immunology, Aichi Medical University School of Medicine, Aichi 480-1195, Japan; ‡Department of Anatomic Pathology and Molecular Diagnostics, Nagoya City University Graduate School of Medical Sciences, Aichi 467-8601, Japan; and §Department of Immunology, University of the Ryukyus, Okinawa, 903-0215, Japan

Received for publication September 26, 2012. Accepted for publication May 1, 2013.

This work was supported by Grants-in-Aid for Young Scientists (A) (22689029 to T.I.), Scientific Research (B) (22300333 to T.I. and R.U.), and Scientific Support Programs for Cancer Research (221S0001 to T.I.) from the Ministry of Education, Culture, Sports, Science and Technology of Japan, Grants-in-Aid from the National Cancer Center Research and Development Fund (23-A-17 to T.I.), and Health and Labour Sciences Research Grants (H22-Clinical Cancer Research-General-028 to T.I. and H23-Third Term Comprehensive Control Research for Cancer-General-011 to T.I. and H.I.) from the Ministry of Health, Labour and Welfare, Japan.

Address correspondence and reprint requests to Dr. Takashi Ishida, Department of Medical Oncology and Immunology, Nagoya City University Graduate School of Medical Sciences, 1 Kawasumi, Mizuho-chou, Mizuho-ku, Nagoya, Aichi 467-8601, Japan. E-mail address: itakashi@med.nagoya-cu.ac.jp

Abbreviations used in this article: ATL, adult T cell leukemia/lymphoma; FSC-H, forward light scatter-height; HTLV-1, human T-lymphotropic virus type 1; sIL-2R, soluble IL-2R; SSC, side scatter-height; Treg, regulatory T.

www.jimmunol.org/cgi/doi/10.4049/jimmunol.1202692

Materials and Methods

Primary human cells

Primary ATL cells were obtained from three individual patients of which patient 1 had chronic-type and patients 2 and 3 were acute. Diagnosis and classification of clinical subtypes of ATL was according to the criteria proposed by the Japan Lymphoma Study Group (22). Mononuclear cells were isolated from blood or lymph node cells with Ficoll-Paque (Pharmacia, NJ). Primary ATL cells were separated using anti-human CD4 microbeads (Miltenyi Biotec, Bergisch Gladbach, Germany) by means of an autoMACS Pro (Miltenyi Biotec). Genotyping of HLA-A, -B, and -C was performed using an HLA-typing Kit (WAKFlow HLA-typing kit; Wakunaga Pharmacy, Hiroshima, Japan). The disease activity of patient 1 was stable; this patient had been carefully observed under a wait-and-see policy for ~4 y prior to sampling. Both patients 2 and 3 received systemic chemotherapies and achieved complete remissions. Patient 2 remained in remission for >18 mo, but in patient 3, ATL relapsed after only 6 mo in remission. Thus, patient 3 subsequently again received systemic chemotherapy for his relapsed ATL. In patients 2 and 3, primary ATL cells were obtained at first diagnosis, and PBMC for CTL expansion were obtained in remission. They were cryopreserved until use. All donors provided informed written consent before sampling according to the Declaration of Helsinki, and the current study was approved by the institutional ethics committees of Nagoya City University Graduate School of Medical Sciences.

Cell lines

ATN-1, MT-1, and TL-Om1 are ATL cell lines, TL-Su, TCL-Kan, and MT-4 are HTLV-1–immortalized lines, and K562 is a chronic myelogenous leukemia blast crisis cell line, as previously described (17).

Expansion of HTLV-1 Tax-specific CTL

PBMC from the ATL patients were suspended in RPMI 1640 (Cell Science and Technology Institute, Sendai, Japan) supplemented with 10% human serum and 0.1 μM Tax epitope peptide (LLFGYPVYV or SFHSLHLLF; Invitrogen, Carlsbad, CA) at a cell concentration of 2.0×10^6/ml. The cells were cultured at 37°C in 5% CO_2 for 2 d, and then an equal volume of RPMI 1640 supplemented with 100 IU/ml IL-2 was added. After subsequent culture for 5 d, an equal volume of ALyS505N (Cell Science and Technology Institute) supplemented with 100 IU/ml IL-2 was added, and the cells were cultured with appropriate medium (ALyS505N with 100 IU/ml IL-2) for 7 d.

Abs, tetramers, and flow cytometry

PE-conjugated HLA-A*02:01/Tax11–19 (LLFGYPVYV) and HLA-A*24:02/Tax301–309 (SFHSLHLLF) tetramers and PE-Cy5–conjugated anti-CD8 mAb (clone, SFCI21Thy2D3) were purchased from MBL (Nagoya, Japan). PE-Cy5–conjugated anti-CD4 mAb (13B8.2) was purchased from Beckman Coulter (Luton, U.K.). Allophycocyanin-conjugated anti-human CD45 mAb (2D1), PE-conjugated anti-CD25 mAb (M-A251), PerCP-conjugated anti-CD4 mAb (SK3), and MultiTEST CD3 FITC/CD8 PE/CD45 PerCP/CD4 APC Reagent were purchased from BD Biosciences (San Jose, CA). For assessing Tax expression, cells were fixed with 10% formaldehyde and then stained with FITC-conjugated anti-Tax mAb Lt-4 (23) or isotype control Ab (A112-3; BD Biosciences), with 0.25% saponin (Sigma-Aldrich, Tokyo, Japan) for 60 min at room temperature. For intracellular IFN-γ staining, the expanded cells including Tax-CTL were cocultured with target cells at 37°C in 5% CO_2 for 2 h after which brefeldin A (BD Biosciences) was added at 2 μg/ml. The cells were then incubated for a further 2 h. Subsequently, they were fixed in 10% formaldehyde and then stained with FITC-conjugated anti–IFN-γ mAb (45.15; MBL) with 0.25% saponin for 60 min at room temperature. Cells were analyzed on a FACSCalibur (BD Biosciences) with the aid of FlowJo software (Tree Star, Ashland, OR).

Quantitative RT-PCR

Total RNA was isolated with RNeasy Mini Kits (Qiagen, Tokyo, Japan). Reverse transcription from the RNA to first-strand cDNA was carried out using High Capacity RNA-to-cDNA Kits (Applied Biosystems, Foster City, CA). *Tax* and *β-actin mRNA* were amplified using TaqMan Gene Expression Assays with the aid of an Applied Biosystems StepOnePlus. The primer set for Tax was as follows: sense, 5′-AAGACCACCAACACCATGGC-3′, and antisense, 5′-CCAAACACGTAGACTGGGTATCC -3′. All values given are means of triplicate determinations.

Animals

NOG mice were purchased from the Central Institute for Experimental Animals and used at 6–8 wk of age. All of the in vivo experiments were performed in accordance with the United Kingdom Coordinating Committee on Cancer Research Guidelines for the Welfare of Animals in Experimental Neoplasia, Second Edition, and were approved by the Ethics Committee of the Center for Experimental Animal Science, Nagoya City University Graduate School of Medical Sciences.

ATL tumor–bearing mouse model, therapeutic setting

CD4-positive primary ATL cells were separated from PBMC of patient 1 and suspended at 1×10^7 cells per 0.2 ml RPMI 1640, which were i.p. inoculated into each of 20 NOG mice. The inoculated ATL cells consisted of pooled cells from several blood samplings. The primary ATL-bearing mice were divided into two groups of 10 each. One group was used for evaluation of ATL cell organ infiltration and to measure levels of human soluble IL-2R (sIL-2R) in sera using the human sIL-2R immunoassay kit (R&D Systems, Minneapolis, MN) 27 d after tumor inoculation. The other group was used for evaluation of survival. Each group was further divided into two groups of five each for autologous Tax-CTL or control (0.2 ml RPMI 1640) injections. Autologous Tax-CTL suspended in 0.2 ml RPMI 1640 were i.p. injected 2 (mononuclear cells, 4.59×10^6/mouse; CD8-positive and HLA-A*24:02/Tax 301–309 tetramer-positive cells, 7.89×10^5/mouse), 7 (3.57×10^6; 9.71×10^5), 12 (3.26×10^6; 5.49×10^5), 20 (3.12×10^6; 5.48×10^5), and 23 d (2.51×10^6; 4.22×10^5) after ATL cell inoculations. Control RPMI 1640 was i.p. injected in the same manner.

PBMC of patient 2, consisting of ~80% of $CD4^+CD25^+$ ATL cells, were suspended in 0.2 ml of RPMI 1640 and i.p. inoculated into each of six NOG mice. The primary ATL-bearing mice were divided into two groups of three each for autologous Tax-CTL or control injections. Autologous Tax-CTL suspended in 0.2 ml RPMI 1640 were i.p. injected 2 (mononuclear cells, 7.50×10^6/mouse; CD8-positive and HLA-A*24:02/Tax 301-309 tetramer-positive cells, 18.1×10^5/mouse), 7 (6.75×10^6; 22.3×10^5), 14 (5.95×10^6; 20.7×10^5), 21 (5.70×10^6; 22.3×10^5), and 23 d (6.04×10^6; 21.3×10^5) after ATL cell inoculations. Control RPMI 1640 was i.p. injected in the same manner. The infiltration of ATL cells into the organs, and the levels of human sIL-2R in the sera 31 d after tumor inoculation were determined.

Lymph node cells of patient 3, consisting of ~90% $CD4^+CD25^+$ ATL cells, were i.p. inoculated into each of six NOG mice in the same manner as for patient 2. Autologous Tax-CTL suspended in 0.2 ml RPMI 1640 were i.p. injected 2 (mononuclear cells, 10.3×10^6/mouse; CD8-positive and HLA-A*24:02/Tax 301–309 tetramer-positive cells, 2.08×10^5/mouse), 7 (5.73×10^6; 7.53×10^5), and 29 d (18.8×10^6; 16.1×10^5) after tumor cell inoculations. Control RPMI 1640 was i.p. injected in the same manner. The infiltration of ATL cells into the organs and the levels of human sIL-2R in the sera 33 d after tumor inoculation were determined.

Immunopathological analysis

H&E staining and immunostaining by anti-CD4 (4B12; Novocastra, Wetzlar, Germany), CD25 (4C9; Novocastra), and CD8 (C8/144B; DakoCytomation, Glostrup, Denmark) was performed on formalin-fixed, paraffin-embedded sections, using a Bond-Max autostainer (Leica Microsystems, Wetzlar, Germany) with the Bond polymer refine detection kit (Leica Microsystems).

Statistical analysis

The differences between groups regarding the percentage of ATL cells in mouse whole blood cells, liver, and spleen cell suspensions and human sIL-2R concentrations in the serum were examined with the Mann–Whitney *U* test. Survival analysis was done by the Kaplan-Meier method, and survival curves were compared using the log-rank test. All analyses were performed with SPSS Statistics 17.0 (SPSS, Chicago, IL). In this study, $p = 0.05$ was considered significant.

Results

Tax expression in ATL cells from patients

The inoculated primary ATL cells from all three patients were positive for CD4 and CD25 (Fig. 1A, *left panel*, Fig. 1C, 1D, *top left panels*). Tax proteins were weakly detected in a subpopulation of ATL cells from all patients by flow cytometry (Fig. 1A, *right two panels*, and Fig. 1C, 1D, *top right two panels*). The *Tax/human β-actin mRNA* levels of the ATL cells from patients 1, 2, and 3, were 0.192 ± 0.005 (SD), 0.492 ± 0.054, and 0.080 ± 0.009, respectively, when the value of TL-Su was set at unity as previously described (17) (Fig. 2D). Although the short time of in vitro culture changes the expression levels of Tax in primary ATL cells (17, 24), the result presented in this study was obtained at the same time as

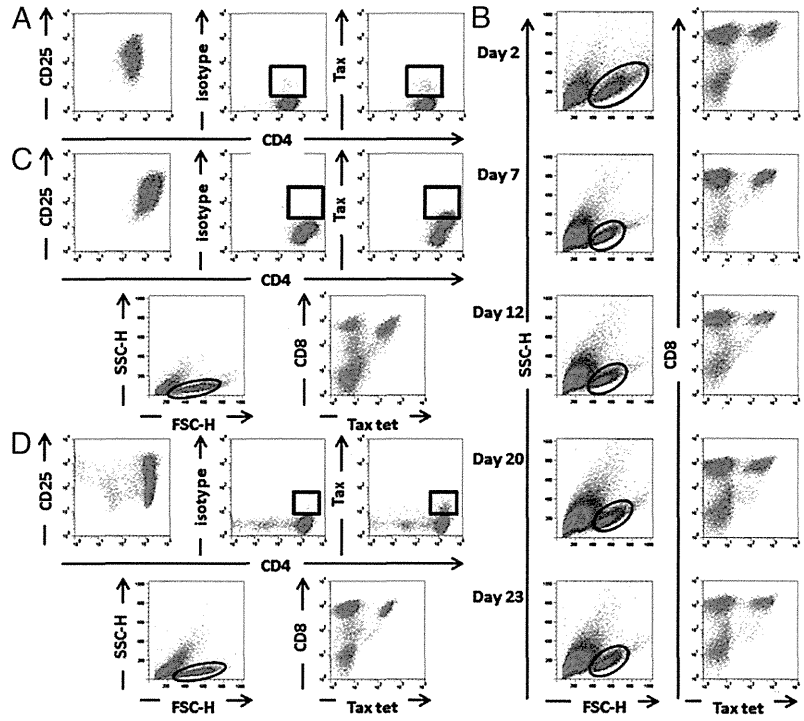

FIGURE 1. Inoculated primary ATL cells and adoptively transferred Tax-specific CTL. (**A**) The inoculated primary ATL cells from patient 1 were positive for CD4 and CD25 (*left panel*). Tax protein was weakly detected in a subpopulation of ATL cells (*middle and right panels*). (**B**) Autologous adoptively transferred Tax-CTL from patient 1 at days 2, 7, 12, 20, and 23, respectively, are presented. The lymphocyte population is determined by FSC-H and SSC-H levels (*left panels*) and plotted to show CD8 and HLA-A*24:02/Tax tetramer positivity (*right panel*). (**C**) The inoculated primary ATL cells from patient 2 were positive for CD4 and CD25 (*top left panel*). Tax protein was weakly detected in a subpopulation of ATL cells (*top right two panels*). Autologous adoptively transferred Tax-CTL from patient 2 are presented. Lymphocyte population is determined by FSC-H and SSC-H levels (*bottom left panel*) and plotted to show CD8 and HLA-A*02:01/Tax tetramer positivity (*bottom right panel*). (**D**) The inoculated primary ATL cells from patient 3 were positive for CD4 and CD25 (*top left panel*). Tax protein was weakly detected in a subpopulation of ATL cells (*top right two panels*). Autologous adoptively transferred Tax-CTL from patient 3 are presented. Lymphocyte population is determined by FSC-H and SSC-H levels (*bottom left panel*) and plotted to show CD8 and HLA-A*24:02/Tax tetramer positivity (*bottom right panel*).

the in vitro experiments were performed, showing Tax-specific CTL responses against autologous ATL cells (Fig. 2A–C).

Adoptively transferred autologous Tax-specific CTL

Flow cytometric analyses of the expanded and adoptively transferred Tax-CTL of patient 1 at days 2, 7, 12, 20, and 23 are presented. The lymphocyte population was identified by forward light scatter-height (FSC-H) and side scatter-height (SSC-H) values (Fig. 1B, *left panels*) and is plotted to show CD8 and HLA-A*24:02/Tax tetramer-positivity (Fig. 1B, *right panel*). Adoptively transferred Tax-CTL from patients 2 and 3 are also shown in Fig. 1C and 1D, *bottom panels*, respectively.

Tax-specific CTL responses against autologous ATL cells in vitro

The adoptively transferred Tax-CTL from patient 1 were cocultured with autologous ATL cells, ATL cell lines, HTLV-1–immortalized lines, or K562, and their responses were evaluated by IFN-γ production in vitro (Fig. 2A, 2D). HLA-A*24:02/Tax301–309 tetramer-positive fractions of these expanded CD8-positive cells produced IFN-γ when cocultured with autologous ATL cells, TL-Su, or ATN-1. These tetramer-positive cells did not respond to MT-1, MT-4, or TCL-Kan. These results indicate that only target cells having both HLA-A*24:02 and Tax were recognized. The tetramer-negative fractions of these expanded CD8-positive cells also produced IFN-γ when stimulated with autologous ATL cells. This suggests that they recognize unidentified Tax-derived epitopes, Ags derived from HTLV-1 components other than Tax, or ATL-related tumor Ags not of viral origin such as cancer testis Ags (25). The tetramer-negative fractions of these expanded CD8-positive cells also produced IFN-γ when stimulated with TCL-Kan. Because both patient 1 and TCL-Kan share HLA-A*02:07, -B*46:01, and -C*01:02, the tetramer-negative cells might be recognizing unidentified Tax-derived epitopes, other HTLV-1 Ags or ATL tumor Ag–derived epitopes presented on a different shared MHC allele. These effector cells did not respond to K562 by IFN-γ production, showing that they had no NK activity.

The adoptively transferred Tax-CTL from patient 2 were tested next. HLA-A*02:01/Tax11–19 tetramer-positive fractions of these expanded CD8-positive cells specifically produced IFN-γ when stimulated with 0.1 μM of the corresponding peptide. These cells also respond to target cells including autologous ATL cells in a manner restricted by Tax expression and the appropriate HLA type as did patient 1 (Fig. 2B, 2D).

The adoptively transferred Tax-CTL from patient 3 were also tested. Although HLA-A*24:02/Tax301–309 tetramer-positive fractions of these expanded CD8-positive cells responded to TL-Su and the corresponding peptide by producing IFN-γ, they did not respond to autologous ATL cells or ATN-1, the Tax expression of which was relatively low (Fig. 2C, 2D).

Macroscopic findings in ATL/NOG mice with cells from patient 1 treated or not treated with adoptive autologous Tax-CTL

Ten primary ATL cell–bearing mice were evaluated for the efficacy of treatment by adoptive transfer of autologous Tax-CTL. The appearance of the mice treated with Tax-CTL and of the controls is shown in Fig. 3, *top* and*bottom panels*, respectively. In general, spleens were much more enlarged in the control mice than in the CTL-treated mice.

Flow cytometric analyses of infiltrating ATL cells in organs of ATL/NOG mice with cells from patient 1

The percentage of CD4-positive ATL cells in whole blood of control NOG mouse 1 was 0.57% (i.e., 0.57% [human CD45-positive population] × 100.0% [human CD4-positive CD8-negative cells] = 0.57%). In control NOG mice 2, 3, 4, and 5 and in Tax-CTL–treated NOG mice 1, 2, 3, 4, and 5, the percentages of ATL cells in whole blood, calculated in the same manner, were 1.57, 2.53, 0.18, and 0.94% and 0.22, 0.17, 0.01, 0.59, and 0.02%, respectively (Fig. 4A). Thus, Tax-CTL treatment significantly reduced the percentage of ATL cells present in the blood of these mice ($p = 0.047$; Fig. 5A, *left panel*).

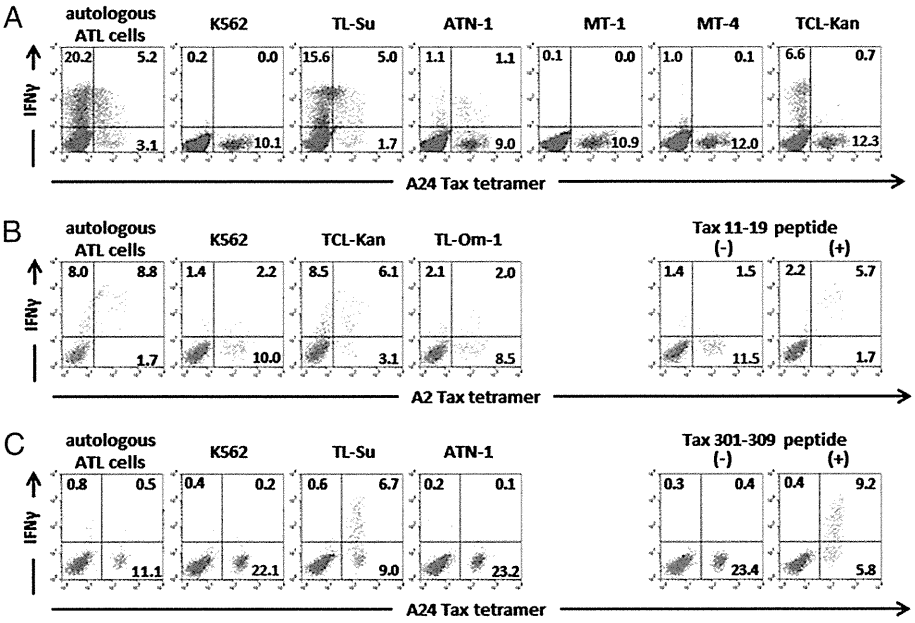

D

	HLA-A		HLA-B		HLA-C		Tax expression (value, SD)	
TL-Su	*11:01	*24:02	*15:01	*40:02	*03:04	*04:01	1.000	
ATN-1	*11:01	*24:02	*54:01	*67:01	*01:02	*07:02	0.010	0.003
MT-1	*11:01	*26:01	*39:01	*40:02	*03:04	*07:02	0.000	
MT-4	*11:01	*31:01	*39:02	*67:01	*07:02	*07:02	2.869	0.260
TL-Om1	*02:01	*02:01	*52:01	*52:01	*12:02	*12:02	0.000	
TCL-Kan	*02:06	*02:07	*46:01	*56:01	*01:02	*07:02	1.597	0.031
K562							-	
patient 1	*02:07	*24:02	*46:01	*52:01	*01:02	*12:02	0.192	0.005
patient 2	*02:03	*31:01	*35:01	*46:01	*01:02	*08:01	0.492	0.054
patient 3	*24:02	*31:01	*40:54	*51:01	*08:03	*14:02	0.080	0.009

FIGURE 2. Tax-specific CTL responses against autologous ATL cells in vitro. (**A**) The adoptively transferred Tax-CTL from patient 1 were cocultured with autologous ATL cells, ATL cell lines, HTLV-1–immortalized lines, or K562 (all CD8 negative) for 4 h. CD8-positive cells are plotted according to HLA-A*24:02/Tax301–309 tetramer-positivity and IFN-γ production, and the percentages in each quadrant are presented in the panels. (**B**) The adoptively transferred Tax-CTL from patient 2 were cocultured with autologous ATL cells, K562, TCL-Kan, or TL-Om1 for 4 h. Tax-CTL were also cultured with or without 0.1 μM cognate peptide (LLFGYPVYV) for 4 h. CD8-positive cells are plotted according to HLA-A*02:01/Tax11–19 tetramer positivity and IFN-γ production, and the percentages in each quadrant are presented in the panels. (**C**) The adoptively transferred Tax-CTL from patient 3 were cocultured with autologous ATL cells, K562, TL-Su, or ATN-1 for 4 h. Tax-CTL were also cultured with or without 0.1 μM cognate peptide (SFHSLHLLF) for 4 h. CD8-positive cells are plotted according to HLA-A*24:02/Tax301–309 tetramer positivity and IFN-γ production, and the percentages in each quadrant are presented in the panels. (**D**) HLA-A, -B, and -C typing of patients 1, 2, and 3. Cell line HLA-A, -B, and -C typing was from our previous study (17). The *Tax/human β-actin mRNA* level of ATL cells from patients 1, 2, and 3, presented as mean value ± SD of triplicate experiments when the value of TL-Su was set as unity. The *Tax/human β-actin mRNA* level of each cell line was from our previous study (17).

The percentages of CD8-positive CD4-negative T cells in the whole blood of Tax-CTL–treated NOG mice 1, 2, 3, 4, and 5 were 0.10, 0.55, 0.00, 0.55, and 0.03%, respectively (Fig. 4A, *bottom panels*).

The percentage of CD4-positive ATL cells in spleen cell suspensions of control NOG mouse 1 was 0.43% (i.e., 0.46% [human CD45-positive population] × 94.35% [human CD4-positive CD8-negative cells] = 0.43%). In control NOG mice 2, 3, 4, and 5 and in Tax-CTL–treated NOG mice 1, 2, 3, 4, and 5, the percentages of ATL cells in the spleen cell suspensions, calculated in the same manner, were 3.24, 1.83, 1.97, and 5.32% and 0.24, 0.09, 0.02, 0.11, and 2.98%, respectively (Fig. 4B). Thus, Tax-CTL treatment significantly decreased the percentage of ATL cells present in the spleen cell suspensions of these mice as well as in the blood ($p = 0.047$; Fig. 5A, *middle panel*). Again, the percentages of CD8-positive CD4-negative T cells in the spleen cell suspensions of Tax-CTL–treated NOG mice 1, 2, 3, 4, and 5 were 0.10, 0.29, 0.02, 0.07, and 2.26%, respectively (Fig. 4B, *bottom panels*).

The percentages of CD4-positive ATL cells in liver cell suspensions were also quantified. In control NOG mouse 1, this value was 0.25% (i.e., 0.26% [human CD45-positive population] × 94.62% [human CD4-positive CD8-negative cells] = 0.25%). In control NOG mice 2, 3, 4, and 5 and in Tax-CTL–treated NOG mice 1, 2, 3, 4, and 5, the percentages of ATL cells in the liver cell suspensions, calculated in the same manner, were 0.50, 0.64, 0.42, and 2.00% and 0.10, 0.05, 0.02, 0.02, and 0.18%, respectively (Fig. 4C). Thus, Tax-CTL treatment also significantly reduced the percentage of ATL cells present in the livers of these mice ($p = 0.009$; Fig. 5A, *right panel*). The percentages of CD8-positive CD4-negative T cells in the liver cell suspensions of Tax-CTL–treated NOG mice 1, 2, 3, 4, and 5 were 0.01, 0.16, 0.02, 0.01, and 0.12%, respectively (Fig. 4C, *bottom panels*).

Microscopy findings in spleens of ATL/NOG mice receiving cells from patient 1 with or without adoptive autologous Tax-CTL therapy

In the control NOG mice, large atypical cells with irregular and pleomorphic nuclei proliferated with a multifocal pattern and

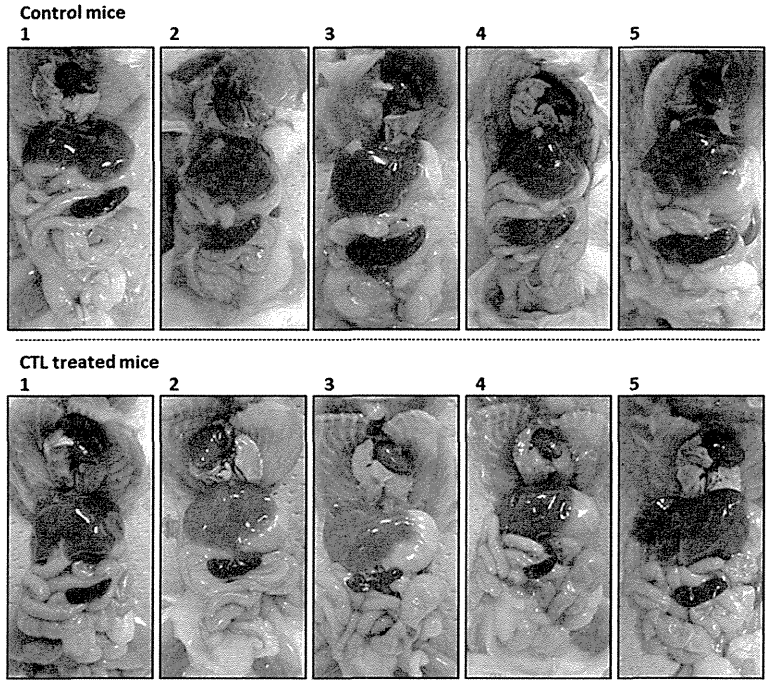

FIGURE 3. Macroscopic findings in ATL/NOG mice with cells from patient 1 with or without adoptive autologous Tax-CTL therapy. The appearance of mice treated with Tax-CTL and of the controls is shown in the *bottom* and *top panels*, respectively. Spleens were much more enlarged in the control mice compared with CTL-treated mice.

replaced normal splenic architecture. Immunopathological analyses of control mouse 4 are shown in Fig. 4D (*three left panels*). The atypical cells were positive for CD4 and CD25 (data not shown), but negative for CD8, consistent with their identity as infiltrating ATL cells. In the Tax-CTL–treated NOG mice, atypical cells proliferated with a patchy pattern. Immunopathological analyses of Tax-CTL-treated NOG mouse 5 are shown in Fig. 4D (*right three panels*). The atypical cells were positive for CD4 and CD25 (data not shown), but negative for CD8, again consistent with ATL cell infiltration. ATL tumor-infiltrating CD8-positive cells were also present, consistent with the flow cytometric analyses showing the presence of CTL (Fig. 4B).

Tax-CTL treatment significantly decreases human sIL-2R concentrations in serum of NOG mice bearing primary ATL cells from patient 1

We measured human sIL2R concentrations in serum as a reliable surrogate marker reflecting ATL tumor burden (26) in the mice. The serum sIL-2R concentrations in control NOG mice 1, 2, 3, 4 and 5 and Tax-CTL–treated NOG mice 1, 2, 3, 4, and 5, were 28,087, 36,924, 34,611, 36,906, and 42,955 and 0, 0, 0, 0, and 1.061 pg/ml, respectively. Thus, Tax-CTL treatment significantly decreased the ATL tumor burden present in these mice ($p = 0.007$; Fig. 5B).

Tax-CTL treatment results in a significant prolongation of survival of primary patient 1 ATL cell–bearing NOG mice

Tax-CTL recipients had a significant benefit in terms of prolongation of survival compared with controls (Fig. 6A; $p = 0.002$). In order to estimate the ATL cell tumor burden during CTL treatment in both groups, flow cytometry analyses of whole blood cells were performed. Thirty-one days after ATL cell inoculation, the percentage of CD4-positive CD8-negative ATL cells in the blood of control NOG mouse 1 was 2.48% (i.e., 2.49% [human CD45-positive population] × 99.60% [human CD4-positive and CD8-negative cells] = 2.48%). In control NOG mice 2, 3, 4, and 5 and in Tax-CTL–treated NOG mice 1, 2, 3, 4, and 5, the percentages of ATL cells in whole blood, calculated in the same manner, were 0.62, 0.56, 0.77, and 1.22% and 0.20, 1.59, 0.11, 0.04, and 0.05%, respectively. At this time, the percentages of CD8-positive CD4-negative T cells in the whole blood of Tax-CTL–treated NOG mice 1, 2, 3, 4, and 5 were 0.32, 1.09, 0.15, 0.19, and 0.07%, respectively (Fig. 6B, *top panels*).

In the same animals, 38 d after ATL cell inoculation, the percentages of CD4-positive ATL cells in the whole blood of control NOG mice 1, 2, 3, and 4 and in Tax-CTL–treated NOG mice 1, 2, 3, 4, and 5 were 1.59, 5.83, 1.79, and 0.88% and 0.08, 2.88, 0.06, 0.00 and 0.04%, respectively. Control NOG mouse 5 sickened and died on day 34 due to ATL progression. At this time, the percentages of CD8-positive CD4-negative T cells in the blood of Tax-CTL–treated NOG mice 1, 2, 3, 4, and 5 were 0.21, 3.72, 0.08, 0.08, and 0.01%, respectively (Fig. 6B, *top, second panel*).

Forty-five days after ATL cell inoculation, the percentage of CD4- and CD25-positive ATL cells in the whole blood of control NOG mouse 1 was 4.60% (i.e., 4.70% [human CD45-positive population] × 97.77% [human CD4-positive and CD25-positive cells] = 4.60%). In control NOG mice 2, 3, and 4 and in Tax-CTL–treated NOG mice 1, 2, 3, 4, and 5, the percentages of ATL cells in whole blood, calculated in the same manner, were 7.07, 1.26, and 1.11 and 0.05, 6.96, 0.04, 0.01, and 0.02%, respectively (Fig. 6B, *bottom, second panel*).

Seventy-nine days after ATL cell inoculation, the percentages of CD4-positive ATL cells in the blood of control NOG mouse 3 and in Tax-CTL–treated NOG mice 1, 2, 3, 4, and 5 were 0.45, and 0.00, 1.27, 0.01, 0.00, and 0.00%, respectively. Control NOG mice 1, 2, and 4 sickened and died on days 47, 47, and 78, respectively, due to ATL progression (Fig. 6B, *bottom panels*). At this time, the percentages of CD8-positive CD4-negative T cells in the whole blood of Tax-CTL–treated NOG mice 1, 2, 3, 4, and 5 were 0.00, 1.11, 0.01, 0.00, and 0.00%, respectively (Fig. 6B, *bottom panels*). Throughout the study, no toxicity attributable to CTL injections was observed in any of the mice that had received cells from patient 1.

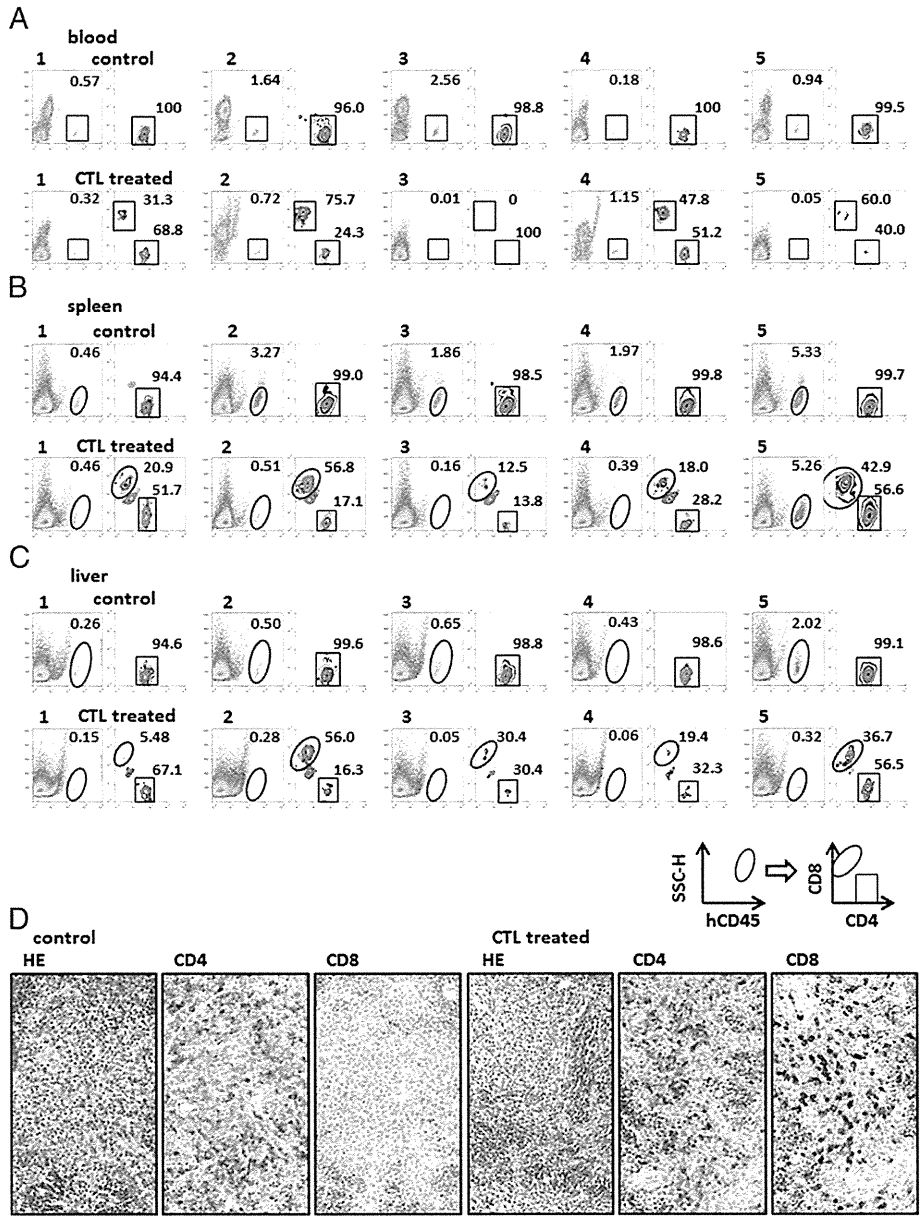

FIGURE 4. Analyses of ATL cell infiltration of cells from patient 1 into the organs. Human CD45-positive cells in ATL/NOG mice plotted to show CD4 and CD8 expression in blood (**A**), spleen (**B**), and liver (**C**). The CD4-positive, CD8-negative cells are ATL cells, and the CD8-positive, CD4-negative cells are the adoptively transferred cells. $CD8^{low}$ populations observed in the spleen (B) and liver (C) cells from CTL-treated mice are nonspecific signals. The percentage of each cell type is indicated in each panel. (**D**) Microscopy findings in spleens of mice with or without adoptive autologous Tax-CTL therapy. Immunopathological analyses of control mouse 4 are shown. The atypical cells were positive for CD4, but negative for CD8, consistent with ATL cell infiltration (*left three panels*). Immunopathological analyses of Tax-CTL–treated NOG mouse 5 indicate atypical cells positive for CD4, but negative for CD8, consistent with ATL cell infiltration. ATL tumor-infiltrating CD8-positive cells were also observed (*right three panels*). No toxicity attributable to CTL injections was observed in any of the mice. Original magnification ×200.

In the blood of CTL-treated mouse 2, not only the CD4-positive ATL cells, but also relatively high levels of CD8-positive cells persisted more than in the other CTL-treated mice. We surmise that the residual ATL cells might persistently stimulate adoptively transferred CD8-positive cells, leading to the expansion of these T cells in the mouse.

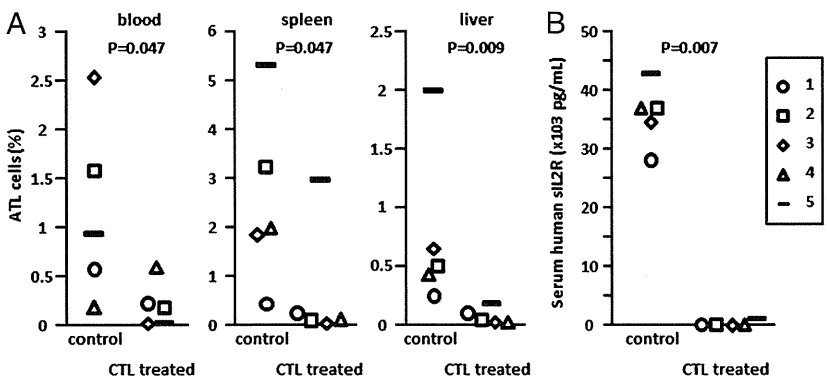

FIGURE 5. Therapeutic efficacy of adoptively transferred autologous Tax-CTL in a NOG mouse bearing primary ATL cells from patient 1. (**A**) The percentages of ATL cells in whole blood, spleen, or liver cell suspensions of each autologous primary ATL-bearing NOG mouse. Tax-CTL treatment led to a significant decrease of ATL cell infiltration into blood, spleen, and liver. (**B**) Human sIL-2R concentration in the serum of each autologous primary ATL-bearing NOG mouse. Tax-CTL treatment significantly decreased human sIL-2R concentrations in serum in the primary ATL cell–bearing NOG mice.

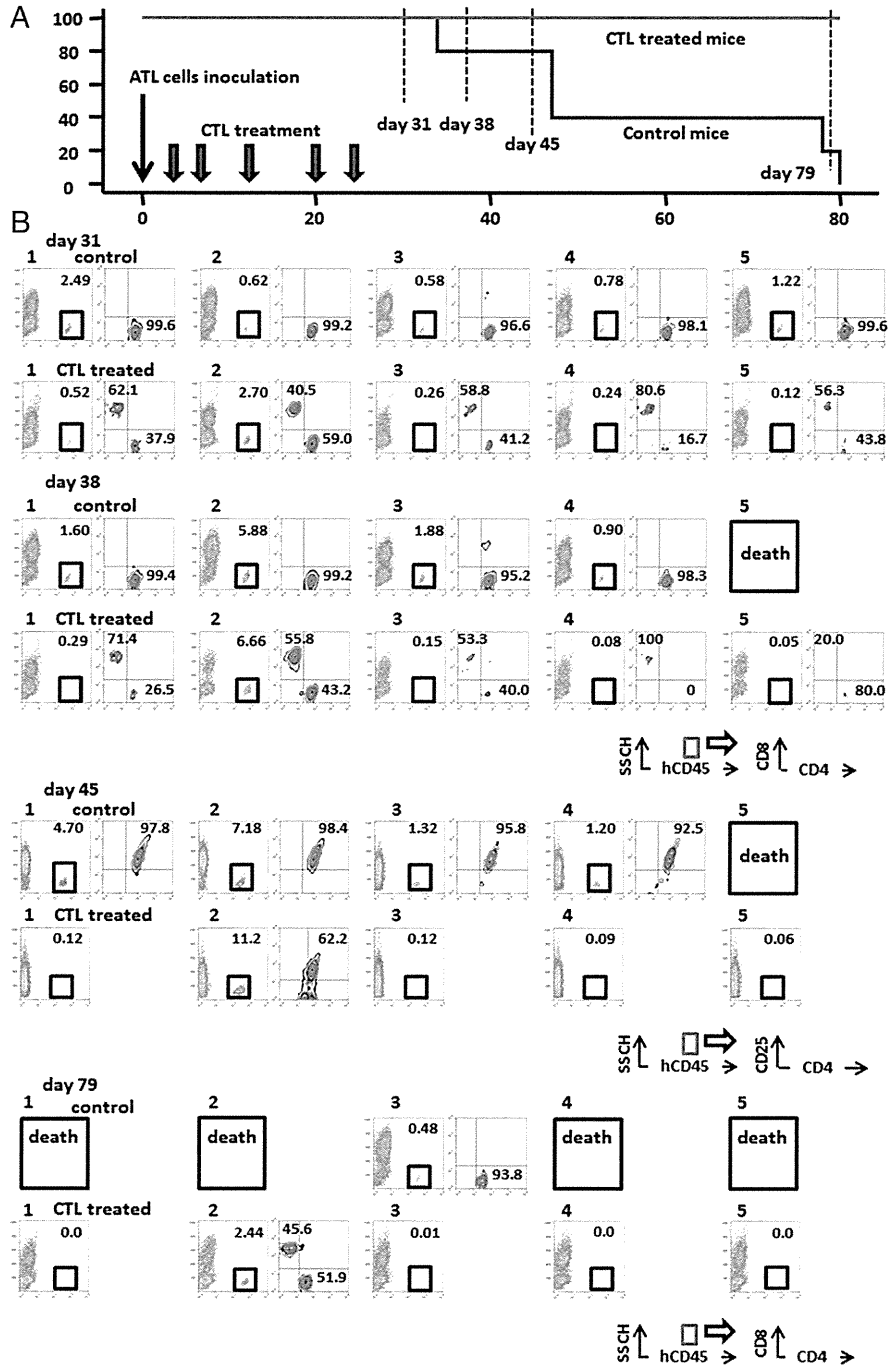

FIGURE 6. Tax-CTL treatment results in a significant prolongation of survival in patient 1 primary ATL cell–bearing NOG mice. Kaplan-Meier survival curves of Tax-CTL–treated and control mice. Tax-CTL recipient mice had a significant prolongation of survival compared with controls ($p = 0.002$) (**A**). In order to assess the ATL cell tumor burden during the CTL treatment in both groups, flow cytometry analyses of whole blood cells were performed (**B**). Thirty-one days after ATL cell inoculation, human CD45-positive cells in the ATL/NOG whole blood are plotted to show CD4 and CD8 expression (*top panel*). Control NOG mouse 5 sickened and died on day 34 due to ATL progression; human CD45-positive cells in the remaining mice are plotted to show CD4 and CD8 expression at day 38 (*second panel from top*). Forty five days after inoculation, human CD45-positive cells are plotted to show CD4 and CD25 expression (*second panel from bottom*). Control NOG mice 1, 2, and 4 sickened and died on days 47, 47, and 78, respectively, due to ATL progression; human CD45-positive cells in the remaining mice are plotted to show CD4 and CD8 expression at day 79 (*bottom panel*). The percentage of each cell type is indicated in each panel. No toxicity attributable to CTL injections was observed in any of the mice.

Therapeutic efficacy of adoptive autologous Tax-CTL in ATL/NOG mice receiving cells from patient 2

ATL cell infiltrations into the organs were evaluated by flow cytometry. The percentage of CD4-positive CD25-positive ATL cells in the whole blood of control NOG mouse 1 was 15.3% (i.e., 16.7% [human CD45-positive population] × 91.5% [human CD4-positive CD25-positive cells] = 15.3%). In control NOG mice 2 and 3 and in Tax-CTL–treated NOG mice 1, 2, and 3, the percentages of ATL cells in whole blood, calculated in the same manner, were 4.4 and 15.3% and 3.3, 5.8, and 5.4%, respectively (Figs. 7A, 8A, *left panel*).

The percentage of CD4-positive CD25-positive ATL cells in the bone marrow of control NOG mouse 1 was 0.71% (i.e., 0.88% [human CD45-positive population] × 80.54% [human CD4-positive CD8-negative cells] = 0.71%). In control NOG mice 2 and 3 and in Tax-CTL–treated NOG mice 1, 2, and 3, the percentages of ATL cells in the bone marrow, calculated in the same manner, were 0.52 and 1.81% and 0.23, 0.11, and 0.13%, respectively (Figs. 7B, 8A, *right panel*).

Immunopathological analyses of liver demonstrated that in the control NOG mice, large atypical cells with irregular and pleomorphic nuclei proliferated with a patchy or focal pattern. The atypical cells were positive for CD4 (Fig. 7C, *top panels*) and CD25 (data not shown), consistent with their being infiltrating ATL cells. In the Tax-CTL–treated NOG mice, there were few areas infiltrated

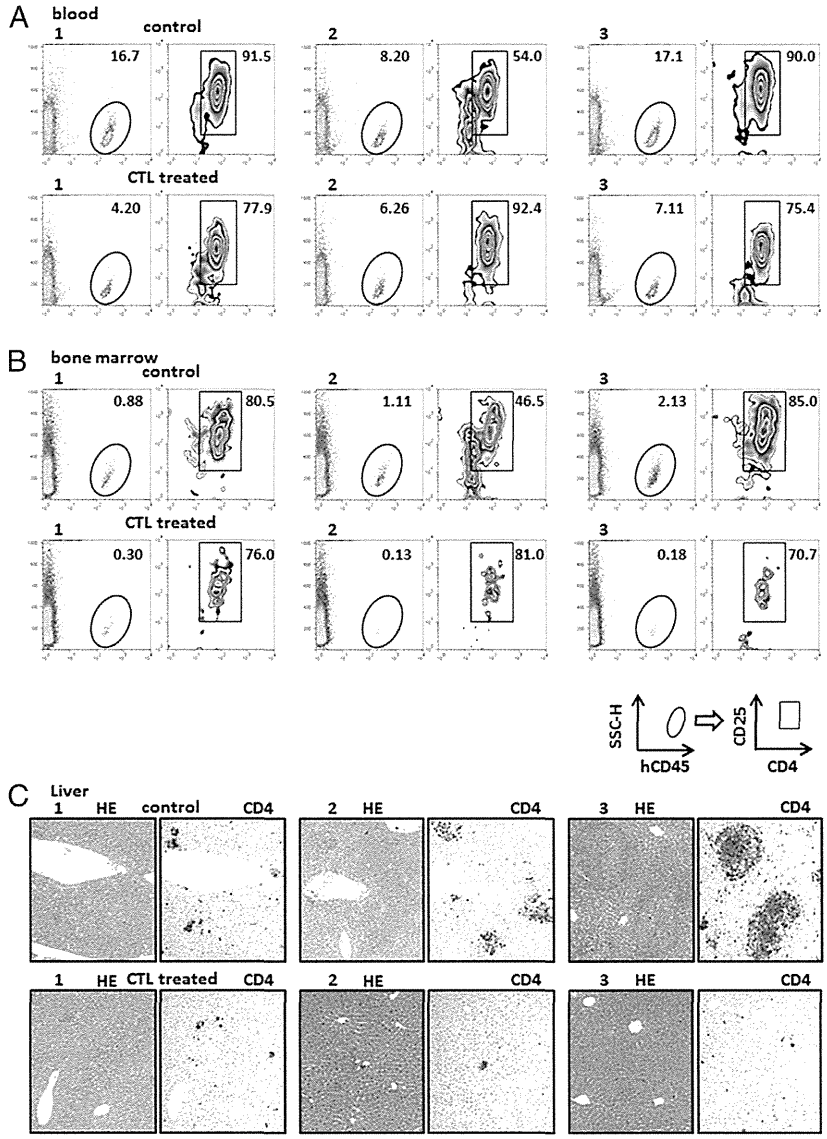

FIGURE 7. Analyses of patient 2 ATL cell infiltration into the organs. Human CD45-positive cells in ATL/NOG mice plotted to show CD4 and CD25 expression in blood (**A**) and bone marrow (**B**). The CD4- and CD25-positive cells are ATL cells. The percentages of each cell type are indicated in each panel. (**C**) Microscopy findings in livers of mice with or without adoptive autologous Tax-CTL therapy. No toxicity attributable to CTL injections was observed in any of the mice. Original magnification ×100.

by atypical cells. Images of CTL-treated mice are shown in Fig. 7C, *bottom panels*. The serum sIL-2R concentrations of control NOG mice 1, 2, and 3 and Tax-CTL–treated NOG mice 1, 2 and 3, were 20,438, 18,487, and 77,555 and 7641, 2101, and 2959 pg/ml, respectively (Fig. 8B). Collectively, autologous Tax-CTL treatment decreased the ATL tumor burden present in these mice. Throughout the study of the mice receiving cells from patient 2, no toxicity attributable to CTL injections was observed in any of the animals.

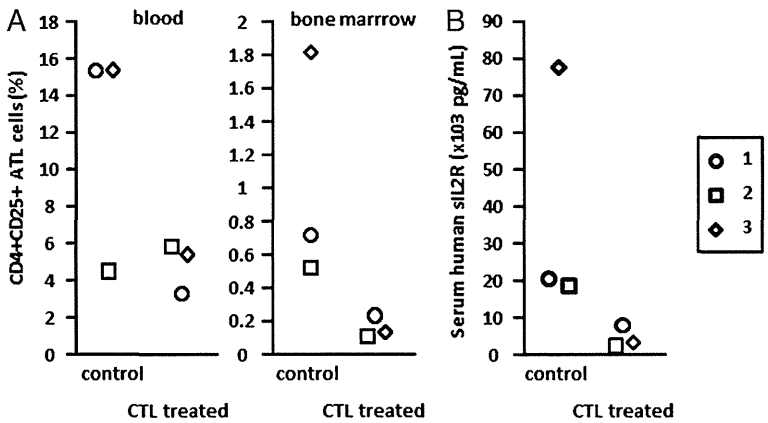

FIGURE 8. Therapeutic efficacy of adoptively transferred autologous Tax-CTL in a patient 2 primary ATL cell–bearing NOG mice. (**A**) The percentages of CD4- and CD25-positive ATL cells in whole blood and bone marrow of each autologous primary ATL-bearing NOG mouse. (**B**) Human sIL-2R concentration in serum of each autologous primary ATL-bearing NOG mouse. Tax-CTL treatment significantly decreased human sIL-2R concentrations in serum in the primary ATL cell–bearing NOG mice.

Therapeutic efficacy of adoptive autologous Tax-CTL in the ATL/NOG mice with cells from patient 3

In this case, Tax-CTL treatment did not show any therapeutic efficacy in controlling CD4-positive CD25-positive ATL cell infiltrations into blood, spleen, liver, or bone marrow, as determined by flow cytometric analyses. There were also no significant differences between CTL-treated and control NOG mice in their serum human sIL-2R concentrations. Again, no toxicity attributable to CTL injections was observed in any of the mice. Collectively, the conclusion in this study must be that autologous Tax-CTL treatment did not decrease the ATL tumor burden present in these mice.

Discussion

In the current study, therapeutic efficacy of adoptive patient-autologous Tax-CTL against two out of three patients' ATL cells was documented in vivo in ATL/NOG mice. In the mouse model with cells from patient 1, infiltration of substantial amounts of CD8-positive T cells into each ATL lesion was observed in the Tax-CTL–treated mice, associated with a significant decrease of ATL cell infiltration into blood, spleen and liver, relative to controls. Tax-CTL treatment significantly decreased human sIL-2R concentrations in the serum (reflecting reduced ATL tumor burden). The efficacy of CTL treatment was also assessed by survival analysis using other ATL/NOG mice. Tax-CTL treatment led to a significant prolongation of survival time compared with control ATL/NOG mice. Adverse events such as organ disorders caused by CTL treatment were not observed in any of the mice. These findings show that Tax-specific CTL infiltrated the tumor site, recognized, and killed autologous ATL cells in mice in vivo. Although Tax expression of the inoculated primary ATL cells from patient 1 (which were cultured in vitro) was low as assessed by flow cytometry (Fig. 1A), potent autologous CTL activity was observed in ATL/NOG mice in vivo. This was partially due to the fact that ATL cells present at the site of active cell proliferation, such as spleen or liver in ATL/NOG mice, expressed substantial amounts of Tax, but it was minimally expressed by the tumor cells in a quiescent state such as in the blood (17). In mice with ATL cells from patient 2, the therapeutic efficacy of adoptive patient-autologous Tax-CTL was also confirmed by decreased ATL cell infiltration into the organs and the levels of human sIL-2R concentrations in the serum. In contrast to these two cases, in mice with cells from patient 3, no therapeutic efficacy was seen in vivo. This is consistent with the finding that the adoptively transferred Tax-CTL did not respond to autologous ATL cells in vitro (Fig. 2C). Although the precise reason for this decreased susceptibility of patient 3 primary ATL cells to autologous Tax-CTL in vitro and in vivo is unclear, it is possible that it may reflect the clinical features of the individual ATL patient. Thus, the clinical manifestation in patient 1, the most susceptible in mice in vivo, was stable disease, with the patient under observation in a watch-and-wait approach. Clinical manifestations of patient 2, moderately susceptible in the mouse model, were aggressive, but the patient did achieve long-term remission. The disease course in patient 3, in contrast, was aggressive, and no long-term remission could be achieved. Thus, although the therapeutic efficacy of Tax-CTL in ATL/NOG mice was different in the three different patients, to the best of our knowledge, this is the first demonstration, to our knowledge, that adoptive therapy with Ag-specific CTL expanded from a cancer patient mediates a potent antitumor effect, leading to significant survival benefit for autologous primary cancer cell–bearing mice in vivo (patient 1). The present study not only provides a strong rationale for exploiting Tax as a possible target for ATL immunotherapy, but also contributes to research supporting the efficacy of adoptive CTL therapy for other types of cancer.

NOG mice have severe, multiple immune dysfunctions, such that human healthy immune cells engrafted into them retain essentially the same functions as in humans (27, 28). In addition, primary human cancer cells also engraft and survive in NOG mice by interacting with murine cells in the microenvironment; thus, NOG mice have contributed to analyzing the pathogenesis of several human cancers, especially hematopoietic malignancies, and evaluating the effects of therapeutic agents (17, 29–32). The primary ATL cells tested in this study could be maintained by serial transplantation in NOG mice, but could not be maintained long-term (>1 mo) in vitro in IL-2–containing media (data not shown). These findings indicate that the ATL cells survived and proliferated in a murine microenvironment-dependent manner. That is to say, the present ATL model should more truly reproduce human ATL in vivo including the tumor microenvironment, compared with any other current models, especially those that use established tumor cell lines.

It is generally accepted that increased regulatory T (Treg) cells in the tumor microenvironment play an important role in tumor escape from host immunity in several different types of cancer (33, 34). Therefore, depletion of Treg cells in the vicinity of tumors is a potentially promising strategy for boosting tumor-associated Ag-specific immunity (35–38). We have shown that a therapeutic anti-CCR4 mAb does deplete Treg cells in vitro (39, 40) and in vivo in humanized mice (27). Furthermore, we confirmed the $CD25^+$ $CD4^+FOXP3^+$ Treg depletion activity mediated by the humanized anti-CCR4 mAb mogamulizumab (KW-0761) in humans (41–44). Therefore, a combination of Tax-CTL adoptive immunotherapy with mogamulizumab to act not only as an anti-ATL agent but also to deplete Treg cells would be promising.

Acknowledgments

We thank Chiori Fukuyama for excellent technical assistance and Naomi Ochiai for excellent secretarial assistance.

Disclosures

Nagoya City University Graduate School of Medical Sciences has received research grant support from Kyowa Hakko Kirin for works provided by T.I. T.I. received honoraria from Kyowa Hakko Kirin. The other authors have no financial conflicts of interest.

References

1. Uchiyama, T., J. Yodoi, K. Sagawa, K. Takatsuki, and H. Uchino. 1977. Adult T-cell leukemia: clinical and hematologic features of 16 cases. *Blood* 50: 481–492.
2. Matsuoka, M., and K. T. Jeang. 2007. Human T-cell leukaemia virus type 1 (HTLV-1) infectivity and cellular transformation. *Nat. Rev. Cancer* 7: 270–280.
3. Poiesz, B. J., F. W. Ruscetti, A. F. Gazdar, P. A. Bunn, J. D. Minna, and R. C. Gallo. 1980. Detection and isolation of type C retrovirus particles from fresh and cultured lymphocytes of a patient with cutaneous T-cell lymphoma. *Proc. Natl. Acad. Sci. USA* 77: 7415–7419.
4. Hinuma, Y., K. Nagata, M. Hanaoka, M. Nakai, T. Matsumoto, K. I. Kinoshita, S. Shirakawa, and I. Miyoshi. 1981. Adult T-cell leukemia: antigen in an ATL cell line and detection of antibodies to the antigen in human sera. *Proc. Natl. Acad. Sci. USA* 78: 6476–6480.
5. Tsukasaki, K., A. Utsunomiya, H. Fukuda, T. Shibata, T. Fukushima, Y. Takatsuka, S. Ikeda, M. Masuda, H. Nagoshi, R. Ueda, et al; Japan Clinical Oncology Group Study JCOG9801. 2007. VCAP-AMP-VECP compared with biweekly CHOP for adult T-cell leukemia-lymphoma: Japan Clinical Oncology Group Study JCOG9801. *J. Clin. Oncol.* 25: 5458–5464.
6. Ishida, T., and R. Ueda. 2011. Antibody therapy for Adult T-cell leukemia-lymphoma. *Int. J. Hematol.* 94: 443–452.
7. Utsunomiya, A., Y. Miyazaki, Y. Takatsuka, S. Hanada, K. Uozumi, S. Yashiki, M. Tara, F. Kawano, Y. Saburi, H. Kikuchi, et al. 2001. Improved outcome of adult T cell leukemia/lymphoma with allogeneic hematopoietic stem cell transplantation. *Bone Marrow Transplant.* 27: 15–20.
8. Ishida, T., M. Hishizawa, K. Kato, R. Tanosaki, T. Fukuda, S. Taniguchi, T. Eto, Y. Takatsuka, Y. Miyazaki, Y. Moriuchi, et al. 2012. Allogeneic hematopoietic stem cell transplantation for adult T-cell leukemia-lymphoma with special em-

phasis on preconditioning regimen: a nationwide retrospective study. *Blood* 120: 1734–1741.
9. Akagi, T., H. Ono, and K. Shimotohno. 1995. Characterization of T cells immortalized by Tax1 of human T-cell leukemia virus type 1. *Blood* 86: 4243–4249.
10. Arnulf, B., M. Thorel, Y. Poirot, R. Tamouza, E. Boulanger, A. Jaccard, E. Oksenhendler, O. Hermine, and C. Pique. 2004. Loss of the ex vivo but not the reinducible CD8+ T-cell response to Tax in human T-cell leukemia virus type 1-infected patients with adult T-cell leukemia/lymphoma. *Leukemia* 18: 126–132.
11. Kannagi, M., K. Sugamura, H. Sato, K. Okochi, H. Uchino, and Y. Hinuma. 1983. Establishment of human cytotoxic T cell lines specific for human adult T cell leukemia virus-bearing cells. *J. Immunol.* 130: 2942–2946.
12. Kannagi, M., S. Harada, I. Maruyama, H. Inoko, H. Igarashi, G. Kuwashima, S. Sato, M. Morita, M. Kidokoro, M. Sugimoto, et al. 1991. Predominant recognition of human T cell leukemia virus type I (HTLV-I) pX gene products by human CD8+ cytotoxic T cells directed against HTLV-I-infected cells. *Int. Immunol.* 3: 761–767.
13. Ohashi, T., S. Hanabuchi, H. Kato, H. Tateno, F. Takemura, T. Tsukahara, Y. Koya, A. Hasegawa, T. Masuda, and M. Kannagi. 2000. Prevention of adult T-cell leukemia-like lymphoproliferative disease in rats by adoptively transferred T cells from a donor immunized with human T-cell leukemia virus type 1 Tax-coding DNA vaccine. *J. Virol.* 74: 9610–9616.
14. Tamai, Y., A. Hasegawa, A. Takamori, A. Sasada, R. Tanosaki, I. Choi, A. Utsunomiya, Y. Maeda, Y. Yamano, T. Eto, et al. 2013. Potential Contribution of a Novel Tax Epitope-Specific CD4+ T Cells to Graft-versus-Tax Effect in Adult T Cell Leukemia Patients after Allogeneic Hematopoietic Stem Cell Transplantation. *J. Immunol.* 190: 4382–4392.
15. Takeda, S., M. Maeda, S. Morikawa, Y. Taniguchi, J. Yasunaga, K. Nosaka, Y. Tanaka, and M. Matsuoka. 2004. Genetic and epigenetic inactivation of tax gene in adult T-cell leukemia cells. *Int. J. Cancer* 109: 559–567.
16. Kannagi, M., N. Harashima, K. Kurihara, T. Ohashi, A. Utsunomiya, R. Tanosaki, M. Masuda, M. Tomonaga, and J. Okamura. 2005. Tumor immunity against adult T-cell leukemia. *Cancer Sci.* 96: 249–255.
17. Suzuki, S., A. Masaki, T. Ishida, A. Ito, F. Mori, F. Sato, T. Narita, M. Ri, S. Kusumoto, H. Komatsu, et al. 2012. Tax is a potential molecular target for immunotherapy of adult T-cell leukemia/lymphoma. *Cancer Sci.* 103: 1764–1773.
18. Hanahan, D., and R. A. Weinberg. 2000. The hallmarks of cancer. *Cell* 100: 57–70.
19. Hanahan, D., and R. A. Weinberg. 2011. Hallmarks of cancer: the next generation. *Cell* 144: 646–674.
20. Sautès-Fridman, C., J. Cherfils-Vicini, D. Damotte, S. Fisson, W. H. Fridman, I. Cremer, and M. C. Dieu-Nosjean. 2011. Tumor microenvironment is multifaceted. *Cancer Metastasis Rev.* 30: 13–25.
21. Ito, M., K. Kobayashi, and T. Nakahata. 2008. NOD/Shi-scid IL2rgamma(null) (NOG) mice more appropriate for humanized mouse models. *Curr. Top. Microbiol. Immunol.* 324: 53–76.
22. Shimoyama, M. 1991. Diagnostic criteria and classification of clinical subtypes of adult T-cell leukaemia-lymphoma. A report from the Lymphoma Study Group (1984-87). *Br. J. Haematol.* 79: 428–437.
23. Lee, B., Y. Tanaka, and H. Tozawa. 1989. Monoclonal antibody defining tax protein of human T-cell leukemia virus type-I. *Tohoku J. Exp. Med.* 157: 1–11.
24. Kurihara, K., N. Harashima, S. Hanabuchi, M. Masuda, A. Utsunomiya, R. Tanosaki, M. Tomonaga, T. Ohashi, A. Hasegawa, T. Masuda, et al. 2005. Potential immunogenicity of adult T cell leukemia cells in vivo. *Int. J. Cancer* 114: 257–267.
25. Nishikawa, H., Y. Maeda, T. Ishida, S. Gnjatic, E. Sato, F. Mori, D. Sugiyama, A. Ito, Y. Fukumori, A. Utsunomiya, et al. 2012. Cancer/testis antigens are novel targets of immunotherapy for adult T-cell leukemia/lymphoma. *Blood* 119: 3097–3104.
26. Motoi, T., T. Uchiyama, H. Uchino, R. Ueda, and K. Araki. 1988. Serum soluble interleukin-2 receptor levels in patients with adult T-cell leukemia and human T-cell leukemia/lymphoma virus type-I seropositive healthy carriers. *Jpn. J. Cancer Res.* 79: 593–599.
27. Ito, A., T. Ishida, H. Yano, A. Inagaki, S. Suzuki, F. Sato, H. Takino, F. Mori, M. Ri, S. Kusumoto, et al. 2009. Defucosylated anti-CCR4 monoclonal antibody exercises potent ADCC-mediated antitumor effect in the novel tumor-bearing humanized NOD/Shi-scid, IL-2Rgamma(null) mouse model. *Cancer Immunol. Immunother.* 58: 1195–1206.
28. Sato, F., A. Ito, T. Ishida, F. Mori, H. Takino, A. Inagaki, M. Ri, S. Kusumoto, H. Komatsu, S. Iida, et al. 2010. A complement-dependent cytotoxicity-enhancing anti-CD20 antibody mediating potent antitumor activity in the humanized NOD/Shi-scid, IL-2Rγ(null) mouse lymphoma model. *Cancer Immunol. Immunother.* 59: 1791–1800.
29. Mori, F., T. Ishida, A. Ito, F. Sato, A. Masaki, H. Takino, M. Ri, S. Kusumoto, H. Komatsu, R. Ueda, et al. 2012. Potent antitumor effects of bevacizumab in a microenvironment-dependent human lymphoma mouse model. *Blood Cancer J.* 2: e67.
30. Ito, A., T. Ishida, A. Utsunomiya, F. Sato, F. Mori, H. Yano, A. Inagaki, S. Suzuki, H. Takino, M. Ri, et al. 2009. Defucosylated anti-CCR4 monoclonal antibody exerts potent ADCC against primary ATLL cells mediated by autologous human immune cells in NOD/Shi-scid, IL-2R gamma(null) mice in vivo. *J. Immunol.* 183: 4782–4791.
31. Sato, F., T. Ishida, A. Ito, F. Mori, A. Masaki, H. Takino, T. Narita, M. Ri, S. Kusumoto, S. Suzuki, et al. 2013. Angioimmunoblastic T-cell lymphoma mice model. *Leuk. Res.* 37: 21–27.
32. Kikushige, Y., F. Ishikawa, T. Miyamoto, T. Shima, S. Urata, G. Yoshimoto, Y. Mori, T. Iino, T. Yamauchi, T. Eto, et al. 2011. Self-renewing hematopoietic stem cell is the primary target in pathogenesis of human chronic lymphocytic leukemia. *Cancer Cell* 20: 246–259.
33. Restifo, N. P., M. E. Dudley, and S. A. Rosenberg. 2012. Adoptive immunotherapy for cancer: harnessing the T cell response. *Nat. Rev. Immunol.* 12: 269–281.
34. Ishida, T., and R. Ueda. 2006. CCR4 as a novel molecular target for immunotherapy of cancer. *Cancer Sci.* 97: 1139–1146.
35. Yao, X., M. Ahmadzadeh, Y. C. Lu, D. J. Liewehr, M. E. Dudley, F. Liu, D. S. Schrump, S. M. Steinberg, S. A. Rosenberg, and P. F. Robbins. 2012. Levels of peripheral CD4(+)FoxP3(+) regulatory T cells are negatively associated with clinical response to adoptive immunotherapy of human cancer. *Blood* 119: 5688–5696.
36. Ishida, T., and R. Ueda. 2011. Immunopathogenesis of lymphoma: focus on CCR4. *Cancer Sci.* 102: 44–50.
37. Finn, O. J. 2008. Cancer immunology. *N. Engl. J. Med.* 358: 2704–2715.
38. Zou, W. 2006. Regulatory T cells, tumour immunity and immunotherapy. *Nat. Rev. Immunol.* 6: 295–307.
39. Ishida, T., T. Ishii, A. Inagaki, H. Yano, H. Komatsu, S. Iida, H. Inagaki, and R. Ueda. 2006. Specific recruitment of CC chemokine receptor 4-positive regulatory T cells in Hodgkin lymphoma fosters immune privilege. *Cancer Res.* 66: 5716–5722.
40. Ishida, T., S. Iida, Y. Akatsuka, T. Ishii, M. Miyazaki, H. Komatsu, H. Inagaki, N. Okada, T. Fujita, K. Shitara, et al. 2004. The CC chemokine receptor 4 as a novel specific molecular target for immunotherapy in adult T-Cell leukemia/lymphoma. *Clin. Cancer Res.* 10: 7529–7539.
41. Yamamoto, K., A. Utsunomiya, K. Tobinai, K. Tsukasaki, N. Uike, K. Uozumi, K. Yamaguchi, Y. Yamada, S. Hanada, K. Tamura, et al. 2010. Phase I study of KW-0761, a defucosylated humanized anti-CCR4 antibody, in relapsed patients with adult T-cell leukemia-lymphoma and peripheral T-cell lymphoma. *J. Clin. Oncol.* 28: 1591–1598.
42. Ishii, T., T. Ishida, A. Utsunomiya, A. Inagaki, H. Yano, H. Komatsu, S. Iida, K. Imada, T. Uchiyama, S. Akinaga, et al. 2010. Defucosylated humanized anti-CCR4 monoclonal antibody KW-0761 as a novel immunotherapeutic agent for adult T-cell leukemia/lymphoma. *Clin. Cancer Res.* 16: 1520–1531.
43. Ishida, T., T. Joh, N. Uike, K. Yamamoto, A. Utsunomiya, S. Yoshida, Y. Saburi, T. Miyamoto, S. Takemoto, H. Suzushima, et al. 2012. Defucosylated anti-CCR4 monoclonal antibody (KW-0761) for relapsed adult T-cell leukemia-lymphoma: a multicenter phase II study. *J. Clin. Oncol.* 30: 837–842.
44. Ishida, T., A. Ito, F. Sato, S. Kusumoto, S. Iida, H. Inagaki, A. Morita, S. Akinaga, and R. Ueda. 2013. Stevens-Johnson Syndrome associated with mogamulizumab treatment of adult T-cell leukemia / lymphoma. *Cancer Sci.* 104: 647–650.

Leukemia Research 37 (2013) 21–27

Contents lists available at SciVerse ScienceDirect

Leukemia Research

journal homepage: www.elsevier.com/locate/leukres

Angioimmunoblastic T-cell lymphoma mice model

Fumihiko Sato[a,b], Takashi Ishida[a,*], Asahi Ito[a], Fumiko Mori[a], Ayako Masaki[a], Hisashi Takino[b], Tomoko Narita[a], Masaki Ri[a], Shigeru Kusumoto[a], Susumu Suzuki[c], Hirokazu Komatsu[a], Akio Niimi[a], Ryuzo Ueda[c], Hiroshi Inagaki[b], Shinsuke Iida[a]

[a] Department of Medical Oncology and Immunology, Nagoya City University Graduate School of Medical Sciences, 1 Kawasumi, Mizuho-chou, Mizuho-ku, Nagoya, Aichi 467-8601, Japan
[b] Department of Anatomic Pathology and Molecular Diagnostics, Nagoya City University Graduate School of Medical Sciences, 1 Kawasumi, Mizuho-chou, Mizuho-ku, Nagoya, Aichi 467-8601, Japan
[c] Department of Tumor Immunology, Aichi Medical University School of Medicine, Nagakute, Aichi 480-1195, Japan

ARTICLE INFO

Article history:
Received 7 May 2012
Received in revised form 26 July 2012
Accepted 11 September 2012
Available online 29 September 2012

Keywords:
Angioimmunoblastic T-cell lymphoma
Follicular helper T cell
BCL6
PD1
NOG mice
Tumor microenvironment

ABSTRACT

We established an angioimmunoblastic T-cell lymphoma (AITL) mouse model using NOD/Shi-*scid*, IL-2Rγ^{null} mice as recipients. The immunohistological findings of the AITL mice were almost identical to those of patients with AITL. In addition, substantial amounts of human immunoglobulin G/A/M were detected in the sera of the AITL mice. This result indicates that AITL tumor cells helped antibody production by B cells or plasma cells. This is the first report of reconstituting follicular helper T (TFH) function in AITL cells in an experimental model, and this is consistent with the theory that TFH cell is the cell of origin of AITL tumor cells.

1. Introduction

Angioimmunoblastic T-cell lymphoma (AITL) represents a distinct clinicopathological entity among nodal peripheral T-cell lymphomas. A complex network of interactions between AITL tumor cells and the various reactive cellular components of the tumor microenvironment forms the clinical and histological features of AITL [1]. Because of its complexity, analysis of the immunopathogenesis of AITL in vitro seems to be impossible. On the other hand, recent advances in the development of novel mouse models, in which human hematopoietic and/or immune systems could be reconstituted, have contributed to analyzing the pathogenesis of various human diseases and evaluating the effects of therapeutic agents [2–6]. In the present study, we aimed to establish a novel AITL mouse model in which both primary tumor cells of human AITL and microenvironmental reactive cells engraft and interact with each other, using NOD/Shi-*scid*, IL-2Rγ^{null} (NOG) mice [7,8] as recipients, and analyzed the immunopathogenesis of AITL.

2. Materials and methods

2.1. Human cells

The donors of tumor cells provided written informed consent before sampling in accordance with the Declaration of Helsinki. The present study was approved by the institutional ethics committee of Nagoya City University Graduate School of Medical Sciences.

2.2. Animals

NOG mice were purchased from the Central Institute for Experimental Animals and used at 6–8 weeks of age. All of the in vivo experiments were performed in accordance with the United Kingdom Coordinating Committee on Cancer Research Guidelines for the Welfare of Animals in Experimental Neoplasia, Second Edition, and were approved by the ethics committee of the Center for Experimental Animal Science, Nagoya City University Graduate School of Medical Sciences.

2.3. Primary AITL cell-bearing mouse model

The affected lymph node cells from two patients with AITL were suspended in RPMI-1640, and intraperitoneally (i.p.) injected into NOG mice. Lymph node cells of AITL patient 1 were injected at a dose of 2.5×10^7 lymph node cells/mouse (total 2 mice), and those of patient 2 were injected at a dose of 4.0×10^6 lymph node cells/mouse (total 3 mice). When mice that had received lymph node cells from patient 1 or 2 became weakened, they were sacrificed at day 34 and 48, respectively.

2.4. Antibodies and flow cytometry

The following antibodies were used for flow cytometry: MultiTEST CD3 (clone SK7) FITC/CD16 (B73.1)+CD56 (NCAM 16.2) PE/CD45 (2D1) PerCP/CD19 (SJ25C1)

* Corresponding author. Tel.: +81 52 853 8216; fax: +81 52 852 0849.
E-mail address: itakashi@med.nagoya-cu.ac.jp (T. Ishida).

0145-2126/$ – see front matter © 2012 Elsevier Ltd. All rights reserved.
http://dx.doi.org/10.1016/j.leukres.2012.09.009

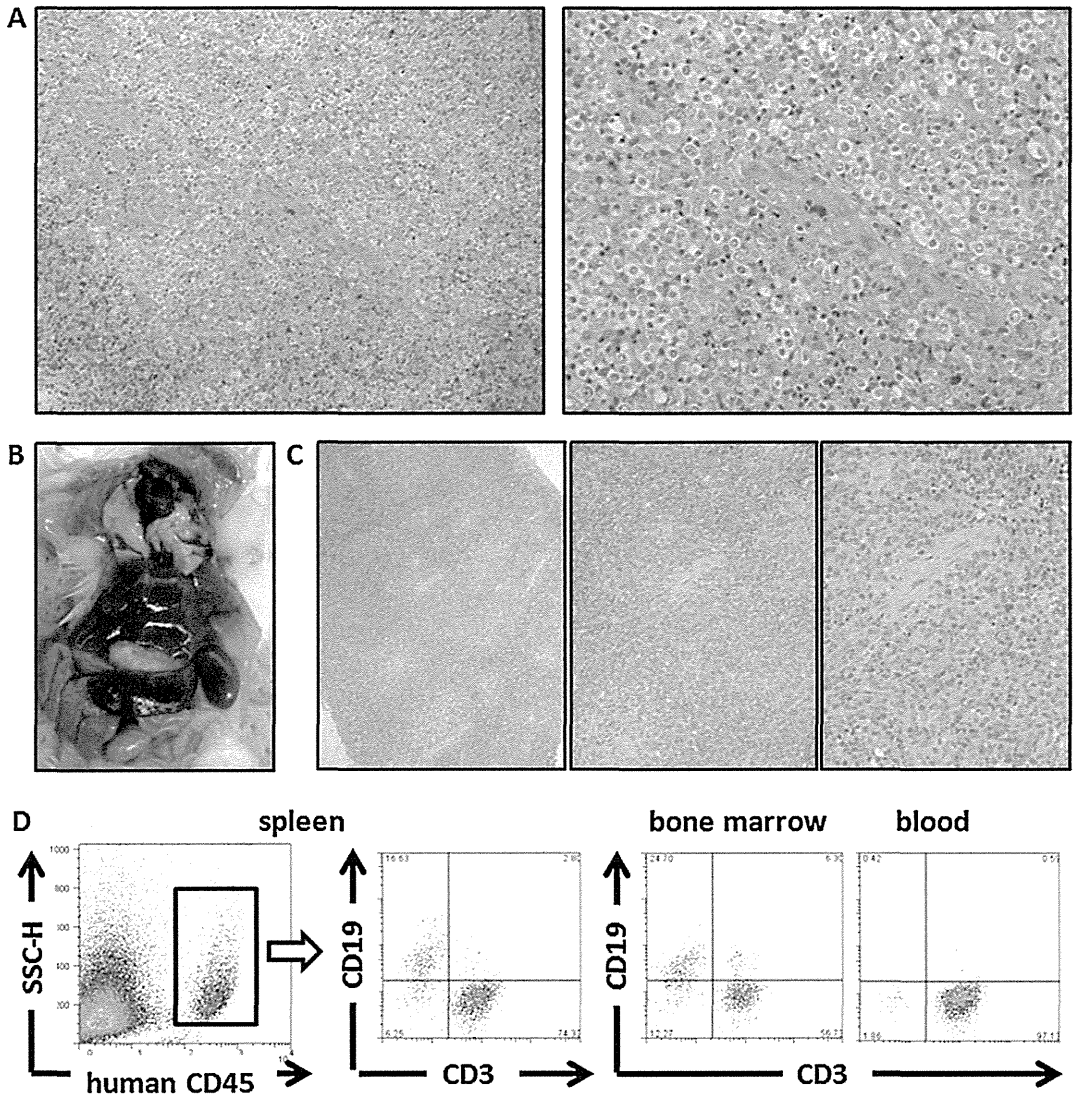

Fig. 1. Primary AITL cell-bearing NOG mouse model. (A) Microscopic images with hematoxylin and eosin staining of the affected lymph node of AITL patient 1 are shown. (B) Macroscopic image of a primary AITL cell-bearing NOG mouse is shown. (C) Sections of the AITL-affected mouse spleen with hematoxylin and eosin staining are shown. (D) The presence of human CD45-positive cells in the infiltrate of the mouse spleen, bone marrow, and blood was determined by flow cytometric analysis of human CD3 and CD19 expression.

APC Reagent, MultiTEST CD3 FITC/CD8 (SK1) PE/CD45 PerCP/CD4 (SK3) APC Reagent. All antibodies were purchased from BD Biosciences (San Jose, CA, USA). Whole blood cells from mice were treated with BD FACS lysing solution (BD Biosciences) for lysing red blood cells. Cells were analyzed by a FACSCalibur (BD Biosciences) with the aid of FlowJo software (Tree Star, Inc., Ashland, OR, USA).

2.5. Immunopathological analysis

Hematoxylin and eosin (HE) staining and immunostaining using antihuman alpha-smooth muscle actin (α-SMA) (1A4; DAKO, Glostrup, Denmark), VEGF-A (sc-152, rabbit polyclonal, Santa Cruz, Heidelberg, Germany), CD3 (SP7; SPRING BIOSCIENCE, Pleasanton, CA, USA), CD20 (L26; DAKO), PD1 (programmed death 1, CD279) (ab52587, Abcam, Cambridge, MA, USA), CD138 (B-B4, Serotec, Raleigh, NC, USA), B cell lymphoma 6 (BCL6) (EP529Y; Epitomics, Burlingame, CA, USA), CD45RO (UCHL1, DAKO), immunoglobulin kappa (KP-53, Novocastra, Newcastle, UK) and lambda light chain (HP-6054, Novocastra) were performed. The presence of Epstein–Barr virus encoded RNA (EBER) was examined by in situ hybridization using EBER Probe (Leica Microsystems, Newcastle, UK) on formalin-fixed, paraffin-embedded sections. Double immunostaining analysis of human CD45RO and human BCL6 was performed as previously described [9]. Briefly, formalin-fixed, paraffin-embedded sections of AITL-affected spleen were immunostained using antibodies against human CD45RO and human BCL6. CD45RO protein in the membrane was visualized in purple (Bajoran purple, Biocare Medical, Concord, CA, USA) and BCL6 protein in the nucleus was visualized in brown (DAB, Leica Microsystems).

2.6. Clonality assay

Clonal assessment of the AITL cells was performed using IdentiClone™ TCRB Gene Clonality Assay (*In vivo*Scribe Technologies, Inc., San Diego, CA, USA) according to the instructions of the manufacturer. Southern blotting analysis of T cell receptor Cβ1 gene was performed at SRL, Inc. (Tokyo, Japan).

2.7. Mouse serum protein

The mouse serum protein fraction was analyzed at SRL, Inc. Human immunoglobulin (Ig) G/A/M in mice serum were also measured at SRL, Inc.

3. Results

3.1. Establishment of the primary AITL cell-bearing NOG mouse model

Microscopic images of the affected lymph node of AITL patient 1 are shown in Fig. 1A. There was marked proliferation of arborizing

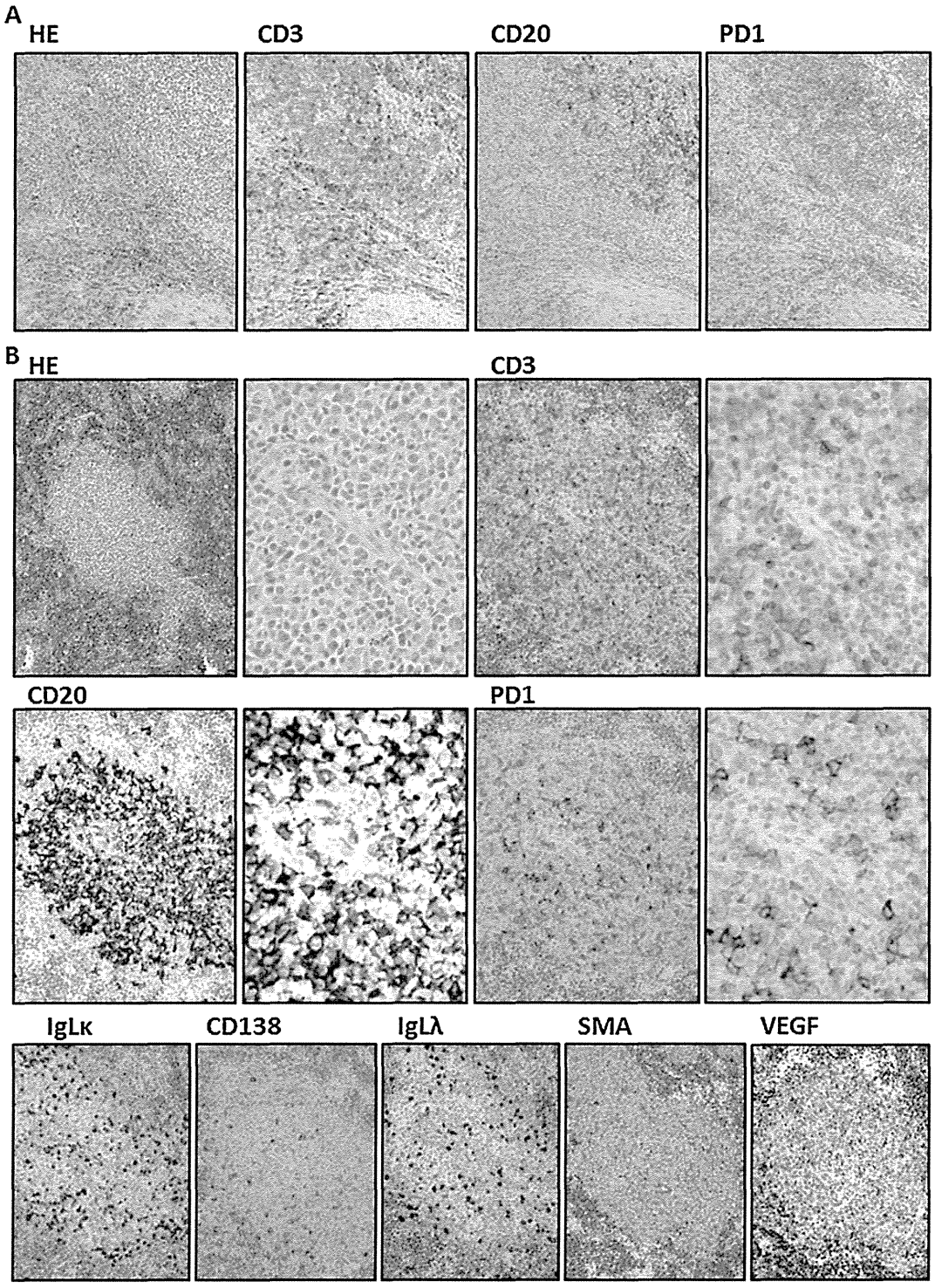

Fig. 2. Immunohistochemical analysis of primary AITL cell-bearing NOG mouse model. (A) Microscopic images with hematoxylin and eosin staining, and staining by anti-CD3, CD20, PD1, and CD138, of the affected lymph node of AITL patient 2 are shown. (B) Immunohistochemical images of sections of the spleen of a primary AITL-affected mouse that had been injected with affected lymph node cells from patient 2, with hematoxylin and eosin staining, and staining by anti-CD3, CD20, PD1, CD138, immunoglobulin kappa and lambda light chain, VEGF-A, and alpha-smooth muscle actin (α-SMA).

high endothelial venules (HEV). There was polymorphic infiltrate composed of small to medium-sized lymphocytes with clear to pale cytoplasm, distinct cell membranes and minimal cytological atypia. The neoplastic cells were admixed with variable numbers of small reactive lymphocytes, eosinophils, plasma cells, and histiocytes. These histological findings are typical of AITL [10]. NOG mice bearing AITL cells from patient 1 presented marked splenomegaly and mild hepatomegaly. The macroscopic appearance of a primary AITL cell-bearing NOG mouse from patient 1 is shown in Fig. 1B. Microscopic analysis revealed that the mice spleen

architectures were partially replaced by the infiltration of small to medium-sized lymphocytes with clear to pale cytoplasm, distinct cell membranes and minimal cytological atypia. The infiltrate also included plasma cells. Marked proliferation of HEV was seen in the spleen (Fig. 1C).

Flow cytometric analysis demonstrated that human CD3-positive T cells as well as CD19-positive B cells infiltrated into the spleen of the mice (Fig. 1D, left 2 panels). Both human T and B cells also infiltrated the mice bone marrow, but only T cells were detected in the blood (Fig. 1D, right 2 panels).

Microscopic images of the affected lymph node of AITL patient 2 are shown in Fig. 2A. There was polymorphic infiltrate composed of small to medium-sized lymphocytes including CD3-positive T cells as well as CD20-positive B cells. Some of the infiltrated cells were positive for PD1, which is known to be expressed on follicular helper T (TFH) cells [11,12] as well as AITL tumor cells [13]. These histological findings are also typical of AITL [10].

NOG mice bearing AITL cells from patient 2 presented marked splenomegaly and mild hepatomegaly. Immunohistochemical analyses of the AITL mice from patient 2 also demonstrated that the mice spleen architectures were partially replaced by the infiltration of small to medium-sized lymphocytes with clear to pale cytoplasm (Fig. 2B, upper left 2 panels). CD3-positive T cells (Fig. 2B, upper right 2 panels) as well as CD20-positive B cells (Fig. 2B, middle left 2 panels) infiltrated the mice spleen. Some of the infiltrated cells were positive for PD1 (Fig. 2B, middle right 2 panels). The infiltrated cells included CD138-positive plasma cells with no slanted distributions of immunoglobulin kappa or lambda light chain (Fig. 2B, lower left 3 panels). EBER-positive cells were not observed in the infiltrate (data not shown). There were abundant SMA-positive blood vessels in the spleen, and the infiltrate included VEGF-producing cells, most of which were AITL tumor cells (Fig. 2B, lower right 2 panels). These observations collectively indicated that the infiltrate consisted of PD1-positive AITL cells, a large number of reactive lymphocytes including both B and T cells, and polyclonal plasma cells, and there was marked vascular proliferation in the spleen. These immunohistological findings in the NOG AITL mice (Figs. 1C and 2B) were nearly identical to those in the respective donor AITL patients (Figs. 1A and 2A).

3.2. Human antibody production in the AITL NOG mice

Given the observation that there were abundant reactive human lymphocytes including B cells and plasma cells in AITL-affected mice spleen, we investigated whether they produced human Ig in the AITL NOG mice. As shown in Fig. 3A, significant Ig fractions and substantial amounts of human IgG/A/M were detected in the AITL mice from both donors. Double immunostaining revealed that human CD45RO- and BCL6-double-positive cells were detected in AITL-affected spleen (Fig. 3B). On the other hand, $CD45RO^{-}BCL6^{+}$ cells were considered to be reactive B cells, because BCL6 is a transcriptional repressor expressed by germinal center B cells [14,15]. These observations collectively indicated that $CD45RO^{+}BCL6^{+}$ AITL tumor cells helped antibody production by B cells or plasma cells. $CD45RO^{+}BCL6^{-}$ cells were also detected in the spleen, and they were reactive T cells with memory phenotype [16].

3.3. Serial transplantations in AITL NOG mice

Suspensions of spleen cells from the mice receiving primary lymph node cells from AITL patient 1 were serially i.p. transplanted into fresh NOG mice. The second NOG mice were sacrificed when they became weakened. The second NOG mice presented marked splenomegaly and mild hepatomegaly (data not shown). Flow cytometric analysis demonstrated that human CD3-positive T cells, including both CD4 and CD8 cells, infiltrated into the mice liver, spleen, and bone marrow. In contrast to the first AITL mice, infiltration of B cells (CD4 and CD8 double negative cells) was not observed (Fig. 4A, left 6 panels). In the subsequent 3rd AITL mice, infiltration of CD8 cells was markedly decreased, and in the 4th AITL mice, the infiltrate of the liver, spleen, and bone marrow consisted of almost exclusively CD4-positive T cells (Fig. 4A, right 6 panels). Along with the disappearance of infiltrating B cells, human Ig was not detected in the sera of 2nd, 3rd and 4th AITL NOG mice (Fig. 4B). Clonality analysis by PCR detected clonal rearrangement of the T cell receptor in the affected lymph node from AITL patient 1 (Fig. 4C, top panel), which was confirmed by Southern blotting analysis of the T cell receptor Cβ1 gene (Fig. 4D, left panels, arrows). Clonality analysis by PCR demonstrated that there were two T cell clones in the spleen cells of the first AITL NOG mice, and the product size of one of these two was the same as that of the original AITL patient (Fig. 4C, upper 2 panels, arrows), indicating that a neoplastic T cell clone from the original AITL patient engrafted and proliferated in the first AITL NOG mice. This observation was confirmed by Southern blotting analysis (Fig. 4D, arrows). The same two T cell clones were detected in the 3rd and 4th AITL mice as those in the 1st AITL mice (Fig. 4C, lower 3 panels, arrows and arrowheads).

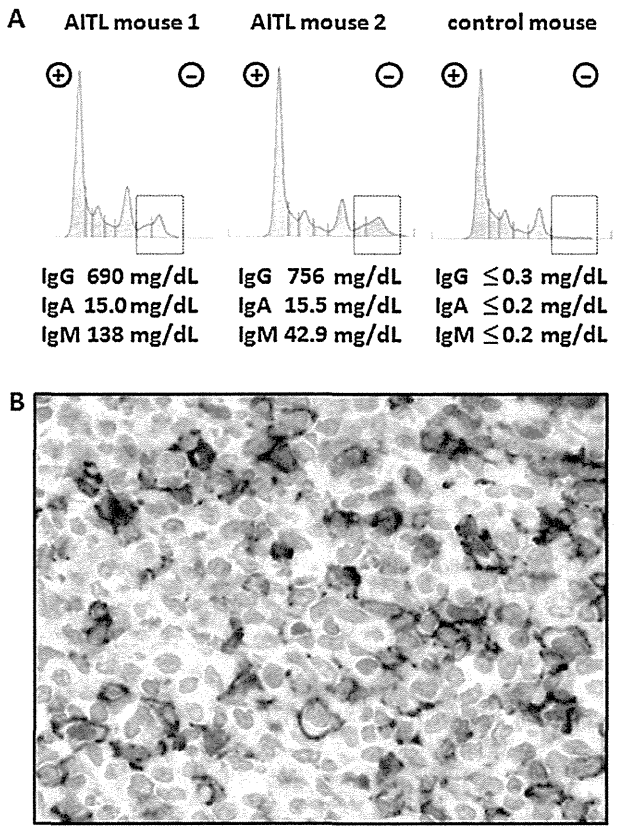

Fig. 3. Human antibody production in the AITL NOG mice. (A) Serum protein fraction of NOG mice that had been injected with affected lymph node cells from AITL patient 1 and 2, and that of a naïve NOG mouse. (B) Double immunostaining analysis for human CD45RO and BCL6 in the AITL-affected mouse spleen. CD45RO in the membrane is visualized in purple and BCL6 in the nucleus is visualized in brown.

3.4. Macroscopic and microscopic findings of 4th AITL mice

The 4th AITL mice presented marked splenomegaly and mild hepatomegaly (Fig. 5A). Mice spleen architectures were almost wholly replaced by the infiltration of small to medium-sized lymphocytes with clear to pale cytoplasm. There was also marked